

Parametric sensitivity analysis of precipitation and temperature based on multi-uncertainty quantification methods in the Weather Research and Forecasting model

DI ZhenHua^{1,2*}, DUAN QingYun^{1,2}, GONG Wei^{1,2}, YE AiZhong^{1,2} & MIAO ChiYuan^{1,2}¹ State Key Laboratory of Earth Surface Processes and Resource Ecology, Faculty of Geographical Science, Beijing Normal University, Beijing 100875, China;² Institute of Land Surface System and Sustainable Development, Faculty of Geographical Science, Beijing Normal University, Beijing 100875, China

Received January 24, 2017; accepted February 22, 2017; published online March 29, 2017

Abstract Sensitivity analysis (SA) has been widely used to screen out a small number of sensitive parameters for model outputs from all adjustable parameters in weather and climate models, helping to improve model predictions by tuning the parameters. However, most parametric SA studies have focused on a single SA method and a single model output evaluation function, which makes the screened sensitive parameters less comprehensive. In addition, qualitative SA methods are often used because simulations using complex weather and climate models are time-consuming. Unlike previous SA studies, this research has systematically evaluated the sensitivity of parameters that affect precipitation and temperature simulations in the Weather Research and Forecasting (WRF) model using both qualitative and quantitative global SA methods. In the SA studies, multiple model output evaluation functions were used to conduct various SA experiments for precipitation and temperature. The results showed that five parameters (P3, P5, P7, P10, and P16) had the greatest effect on precipitation simulation results and that two parameters (P7 and P10) had the greatest effect for temperature. Using quantitative SA, the two-way interactive effect between P7 and P10 was also found to be important, especially for precipitation. The microphysics scheme had more sensitive parameters for precipitation, and P10 (the multiplier for saturated soil water content) was the most sensitive parameter for both precipitation and temperature. From the ensemble simulations, preliminary results indicated that the precipitation and temperature simulation accuracies could be improved by tuning the respective sensitive parameter values, especially for simulations of moderate and heavy rain.

Keywords Multi-uncertainty quantification methods, Qualitative parameters screening, Quantitative sensitivity analysis, Weather Research and Forecasting model

Citation: Di Z H, Duan Q Y, Gong W, Ye A Z, Miao C Y. 2017. Parametric sensitivity analysis of precipitation and temperature based on multi-uncertainty quantification methods in the Weather Research and Forecasting model. *Science China Earth Sciences*, 60: 876–898, doi: 10.1007/s11430-016-9021-6

1. Introduction

Mesoscale numerical weather prediction (NWP) models have become indispensable tools to investigate complex weather processes. However, the outputs of NWP models usually contain errors or biases compared with real weather data (Glahn

and Lowry, 1972; Carter et al., 1989; Allen et al., 2000; Orrell et al., 2001; Danforth et al., 2007). Three factors affect the simulation error of a model: the accuracy of the initial and boundary conditions, the realism of the model physical process representations, and the reasonableness of the model parameters.

Errors in initial conditions were identified in the early stage of NWP model construction (Charney, 1951; Lorenz, 1963).

* Corresponding author (email: zhdi@bnu.edu.cn)

Multiple case studies showed that model prediction accuracy was very sensitive to errors in initial values (Nitta and Ogura, 1972; Zhang and Fritsch, 1986; Zou and Kuo, 1996; Charlton et al., 2004). In addition to initial value error, the effect of lateral boundary error on NWP model forecasting has also been studied (Bontoux et al., 1980; Collins and Allen, 2002). Much effort has been focused on developing data assimilation techniques to reduce errors in initial and lateral boundary conditions. Common data assimilation methods, including the ensemble Kalman filter, three- and four-dimensional variational assimilation, and the ensemble transformed Kalman filter, have been packaged into the NWP model to improve forecasting accuracy (Barker et al., 2004; Wang et al., 2008; Huang et al., 2009; Jia et al., 2013; Liu et al., 2013; Sun et al., 2015).

Along with the increasing number of observational tools (e.g., electronic instruments, radiosonde, radar, and satellites), people have expanded their understanding of real weather physical processes. Moreover, modular structural description of physical processes promotes further development of the NWP model. The model divides the integrated physical processes into multiple single sub-physical processes, each of which is described using a single sub-model developed by groups with different expertise. However, some gaps still exist in the understanding of certain physical mechanisms and the descriptions of the sub-grid processes, and therefore the sub-models are usually represented by different parameterization schemes (Chou and Suarez, 1994; Walko et al., 1995; Hong and Pan, 1996; Mlawer et al., 1997; Chen and Dudhia, 2001; Grell and Dévényi, 2002; Hong et al., 2004; Kain, 2004; Kusaka and Kimura, 2004; Hong and Lim, 2006; Pleim, 2006; Thompson et al., 2008; Chen et al., 2011). The Weather Research and Forecasting (WRF) model (Skamarock et al., 2008) is a representation of NWP models with a modular structure and has multiple parameterization schemes to describe various physical modular processes. The influence of the choice of different parameterization schemes for the same sub-physical process on the predictive results of the WRF model has been widely studied (Ruiz et al., 2007; Gilliam and Pleim, 2010; Kim et al., 2011; Nasrollahi et al., 2012; Chen et al., 2014).

The specification of NWP model parameters is another significant factor impacting model performance (Qiu and Chou, 1988). There are various ways to estimate parameter values. For some parameters (e.g., density, acceleration of gravity) that have specific physical meanings, the values are identified by observational experiments or theoretical calculation. However, the true values of most parameters are unknown and hard to obtain. Some of these parameters have been loosely calibrated by “trial and error” (Allen, 1999; Knutti et al., 2002), which is subjective and constrained by the experience of the researchers. A more objective parameter specification approach is to use an inverse method that fits the

simulated output to the corresponding observation by repeatedly adjusting the model parameter values. The advantage of the inverse method is its ease of implementation; it considers the complex model as a “black box” during parameter optimization. Some inverse methods, such as Markov chain Monte Carlo, genetic algorithms, and multiple very fast simulated annealing, have been widely used to estimate parameters for NWP and climate models (Jackson et al., 2004; Niska et al., 2005; Villagran et al., 2008; Medvigy et al., 2010; Solonen et al., 2012; Yang et al., 2012). Data assimilation, as a type of inverse method, has also been used to estimate the parameter values of climate models (Annan et al., 2005; Kondrashov et al., 2008; Schirber et al., 2013). However, the disadvantage of inverse methods is that they require a large number of model runs to identify the optimal parameter values, especially for models with dozens of parameters. When the inverse method is used to estimate the parameters of the complex NWP model because of its high computation cost and many adjustable parameters, the computations encounter bottlenecks. Therefore, identifying a small number of important parameters to be optimized greatly reduces the number of model runs needed for parameter estimation.

Sensitivity analysis (SA) is commonly used to identify a small number of important parameters (also called sensitive parameters) that exert a significant impact on model outputs (Saltelli et al., 2004). Many parametric SA studies have been carried out on the NWP and other climate models (Gilmore et al., 2004; Liu et al., 2004; Hong et al., 2006; Bellprat et al., 2012; Johannesson et al., 2014; Zou et al., 2014; Qian et al., 2015; Yang et al., 2015). These have usually been classified into three cases. (1) The model simulations for parametric SA experiments were implemented based on a low resolution of approximately 50 to 100 km (e.g., Liu et al., 2004; Bellprat et al., 2012; Johannesson et al., 2014). For high-resolution model simulations (e.g., several kilometers), conventional quantitative SA methods, which require tens of thousands of model runs, are not suitable for parametric SA experiments. Therefore, more effective SA methods (i.e., qualitative SA methods) are needed to conduct parametric SA experiments. (2) The adjustable parameters used for SA experiments were derived from a single physical process scheme (e.g., Gilmore et al., 2004; Hong et al., 2006; Zou et al., 2014; Yang et al., 2015), and therefore the analyzed model parameters were fewer (usually five to eight parameters). Fewer SA studies were therefore required to conduct parametric screening experiments for all physical processes in the NWP model. (3) The three steps for conducting an SA experiment include input parameter sampling, determining the model output errors of all samples, and applying the SA method. For a certain model output variable (e.g., 24-hourly accumulated precipitation), parametric SA experiments were usually conducted using a single SA method (Di et al., 2015), which might have introduced some bias into the results for sensitive parameters.

Therefore, multiple SA methods (especially qualitative and quantitative methods) are required to obtain more reasonable results for sensitive parameters. In addition, various model output-evaluated functions consisting of model output variables and evaluation metrics are used to conduct SA experiments, making the results for the sensitive parameters more comprehensive.

This study systematically explores the sensitivity of the WRF model parameters to high-resolution precipitation and temperature simulation results using qualitative and quantitative SA methods. Two metrics, the threat score (TS) and the root mean square error (RMSE), were used to evaluate precipitation simulation errors for parametric SA experiments, and RMSE was also used to evaluate temperature simulation errors. The precipitation output variables included 6-hourly and 24-hourly accumulated precipitation amounts, and the temperature output variables included 3-hourly average, 24-hourly average, 24-hourly maximum, and 24-hourly minimum temperature values. The errors in the various output variables evaluated by the two metrics and the various SA methods were combined to conduct various parametric SA experiments, producing more comprehensive and reasonable SA results for the WRF parameters.

2. Methodology

2.1 Model configuration and weather event selection

2.1.1 WRF model configuration for the study area

The Advanced Research Weather Research and Forecasting model (WRF-ARW) (Skamarock et al., 2008), Version 3.6.1

(<http://www2.mmm.ucar.edu/wrf/users>), was used in this study. The study area was the Greater Beijing Area (the d02 area in Figure 1) in North China. To obtain more accurate simulation results for d02, a two-grid horizontally nested simulation area was designed. The outer layer (the d01 area in Figure 1) had a horizontal resolution of 9 km and contained 202×145 horizontal grid cells. The inner layer (the d02 area in Figure 1) had a horizontal resolution of 3 km and contained 180×153 horizontal grid cells. Thirty-eight sigma vertical levels from the surface to 50 hPa were defined for the outer and inner layers. The uniform time step was 60 seconds.

The physical parameterization schemes used adhered to the operational setup of the Beijing Meteorological Bureau: the Monin-Obukhov surface layer scheme (Dudhia et al., 2001), the Kain-Fritsch Eta cumulus scheme (Kain, 2004), the WSM six-class Graupel microphysics scheme (Hong and Lim, 2006), the RRTM longwave radiation scheme (Mlawer et al., 1997), the Dudhia shortwave radiation scheme (Stephens et al., 1984; Dudhia, 1989), the unified Noah land-surface model (Chen and Dudhia, 2001), and the Yonsei University planetary boundary layer scheme (Hong and Pan, 1996). The Kain-Fritsch Eta cumulus scheme was not applied to the inner-layer simulation due to its finer spatial resolution of 3 km; however, it was used for the outer-layer simulation with a spatial resolution of 9 km.

Meteorological data, including surface and radiative flux data with a Gaussian T382 spatial resolution and 6-hour interval and three-dimensional pressure level data with 0.5° spatial resolution and a 6-hour interval derived from Climate Forecast System Reanalysis data (CFSR, <http://nomads.nccdc.noaa.gov/data.php?name=access#cfsr>), were

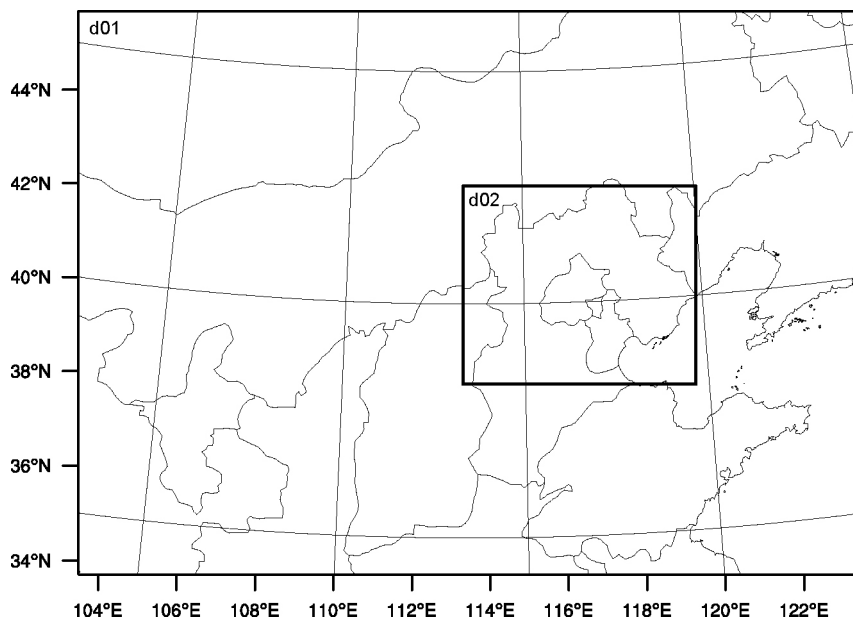


Figure 1 Two-grid simulation domain, with the outer layer (d01) being North China and the inner layer (d02) being the Greater Beijing Area.

used to drive the WRF model as initial and lateral boundary fields.

2.1.2 Selection of rainy and sunny events

To obtain more reasonable parametric SA results for the WRF model, rainy and sunny events were selected to conduct parametric SA experiments for precipitation and temperature, respectively. Figure 2 shows the grid-averaged daily accumulated precipitation amounts for the Greater Beijing Area in the summer season (June, July, and August) from 2008 to 2010. As indicated by the boxes in Figure 2, nine rainy events (marked as events (a)–(i)) and nine rainless events (also called sunny events, marked as events (a)–(i)) were simulated to analyze the parameter sensitivity of the WRF model to precipitation and 2-meter air temperature, respectively. Each of the 18 events spanned two days. A complete run of the WRF simulation for the nine events would have consumed approximately 400 CPU hours; hence, it was impractical to conduct the tens of thousands of WRF runs required by regular quantitative SA methods. Therefore, three qualitative SA methods that required fewer parameter samples and a quantitative SA

method based on a response surface model were used in this study to analyze the parametric sensitivity of the highly complex, dynamic WRF model.

2.2 Adjustable parameters in the six physical parameterization schemes

Based on the list of adjustable parameters and the parametric SA results from Di et al. (2015), the most insensitive parameter was removed, and a new parameter related to mineral thermal conductivity was added. The cumulus scheme was not included in the simulations for the Greater Beijing Area (the d02 area in Figure 1) in the WRF model configuration because the effects of the cumulus scheme from the outer layer on simulations of the inner layer are usually weak. Therefore, the parameter sensitivities from the cumulus scheme were not considered in the inner-layer simulations. Finally, eighteen parameters from six physical schemes of the WRF model, listed in Table 1, were selected to analyze their effects on precipitation and temperature simulation results over the Greater Beijing Area.

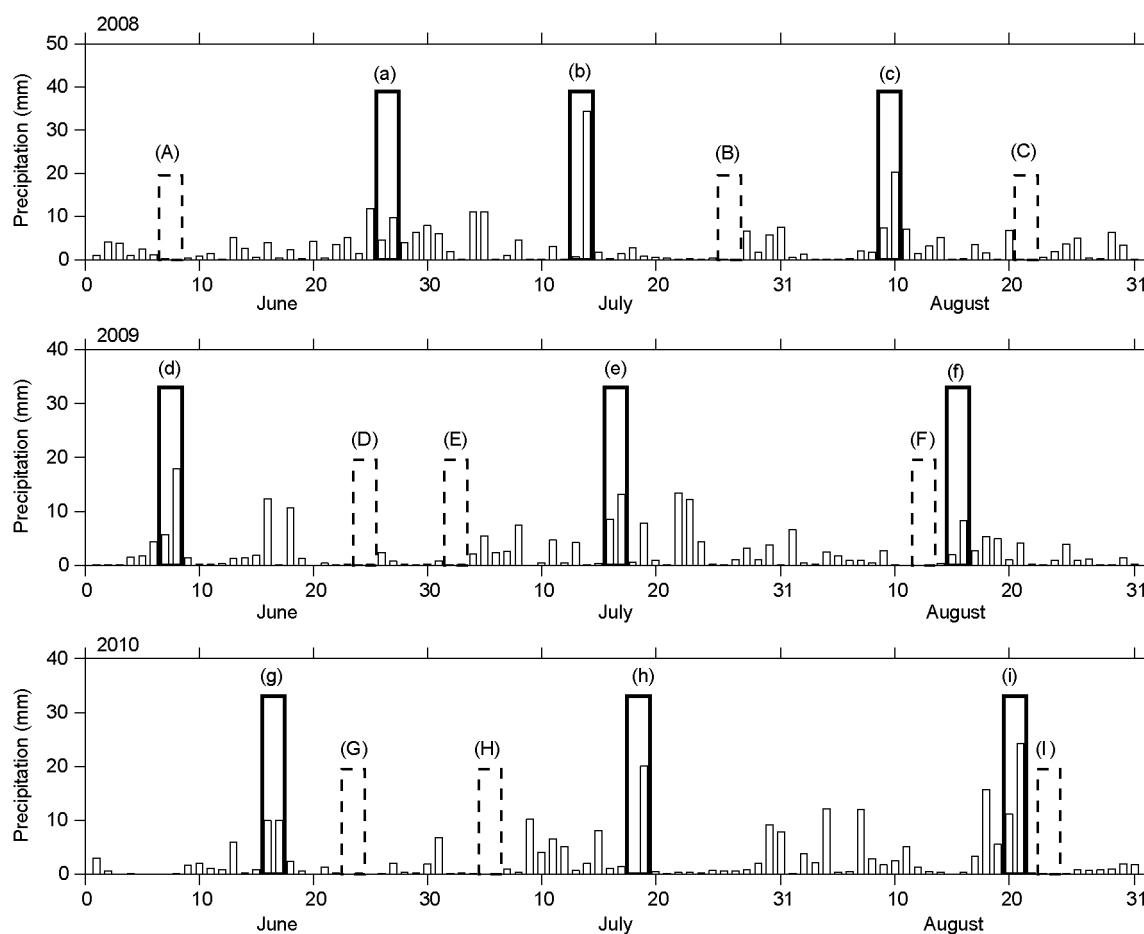


Figure 2 Grid-averaged daily accumulated precipitation amounts in summer (June, July, and August) from 2008 to 2010 in the Greater Beijing Area. The nine two-day rainy events are framed by black boxes with solid lines and indexed from (a) to (i). The nine two-day sunny events are framed by black boxes with dashed lines and marked from (A) to (I).

Table 1 Adjustable parameters and their variability ranges for the WRF model

Index	Scheme	Parameter	Default	Range	Description	
P1	Surface layer (module_sf_sfclay.F)	xka	2.4×10^{-5}	$[1.2 \times 10^{-5}, 5 \times 10^{-5}]$	Parameter for heat/moisture exchange coefficient (s m^{-2})	
P2		czo	0.0185	[0.01, 0.037]	Coefficient for converting wind speed to roughness length over water	
P3	Microphysics (module_mp_wsm6.F)	ice_stokes_fac	14900	[8000, 30000]	Scaling factor applied to ice fall velocity (s^{-1})	
P4		n0r	8×10^6	$[5 \times 10^6, 1.2 \times 10^7]$	Intercept parameter of rain (m^{-4})	
P5		dimax	5×10^{-4}	$[3 \times 10^{-4}, 8 \times 10^{-4}]$	Limiting maximum value for the cloud-ice diameter (m)	
P6		peaut	0.55	[0.35, 0.85]	Collection efficiency for cloud to rain autoconversion	
P7	Short wave radiation (module_ra_sw.F)	cssca	1×10^{-5}	$[5 \times 10^{-6}, 2 \times 10^{-5}]$	Scattering tuning parameter ($\text{m}^2 \text{kg}^{-1}$)	
P8	Longwave (module_ra_rrtm.F)	secang	1.66	[1.55, 1.75]	Diffusivity angle for cloud optical depth computation	
P9	Land surface (module_sf_noahslm.F)	hksati	1	[0.5, 2]	Multiplier for hydraulic conductivity at saturation	
P10		porsl	1	[0.5, 2]	Multiplier for the saturated soil water content	
P11		phi0	1	[0.5, 2]	Multiplier for minimum soil suction	
P12		bsw	1	[0.5, 2]	Multiplier for Clapp and Hornberger “b” parameter	
P13		thk0	2	[1, 4]	Thermal conductivity of other minerals	
P14	Planetary Boundary Layer (module_bl_ysu.F)	brcr_sbrob	0.3	[0.15, 0.6]	Critical Richardson number for the boundary layer of water	
P15		brcr_sb	0.25	[0.125, 0.5]	Critical Richardson number for the boundary layer of land	
P16		pfac	2	[1, 3]	Profile shape exponent used to calculate the momentum diffusivity coefficient	
P17		bfac	6.8	[3.4, 13.6]	Coefficient for Prandtl number at the top of the surface layer	
P18		sm		15.9	[12, 20]	Counter-gradient proportional coefficient of non-local momentum flux

2.3 Sampling approach

Without information on prior parameter distributions, it was assumed that the parameters followed a uniform probability distribution according to maximum entropy or minimum relative entropy theory (Woodbury and Ulrych, 1993; Hou and Rubin, 2005). To approximate the parameter probability distributions, a sampling of the parameter space was conducted. Many sampling approaches are available, including Monte Carlo, fractional factorial, full factorial (Box et al., 2005), Box-Behnken (Box and Behnken, 1960), central composite (Box and Wilson, 1951), Latin hypercube (Mckay et al., 2000), symmetric Latin hypercube (Kenny et al., 2000), and quasi-Monte Carlo (QMC) (Halton and Smith, 1964; Sobol', 1967; Caffisch, 1998). However, not all sampling methods are suitable for uniform sampling of the high-dimensional parameter space of the WRF model. For instance, the number of samples required by the full factorial approach is exponentially proportional to the dimensionality of the parameter space, which means that the WRF model with 18 adjustable parameters and 10 intervals in each parameter range would require 10^{18} samples to approximate the uniformity of the parameter space. Obviously, it is impossible to perform 10^{18} corresponding simulations using the

WRF model to conduct SA experiments. A highly efficient uniform sampling approach should have good space-filling capability with relatively few samples, which would be very useful for the WRF model because it requires huge computational resources. The uniformities of different sampling approaches with the same sample size were compared, and the QMC method was chosen as one of the most efficient uniform sampling approaches (Hou et al., 2012; Wang et al., 2014; Gong et al., 2015; Qian et al., 2015). Therefore, the QMC method was used in this study to produce parametric samples from the 18-dimensional adjustable parameter space for the WRF model.

2.4 Evaluation metrics

To avoid the impact of observation errors on the parametric SA results, the evaluation metric in the SA experiments measured the error of the simulation results of the WRF model with perturbed parameter values by comparing them with the simulation results of the WRF model with the default parameter values. Instead of observed data, the simulation results of the WRF model with the default parameter values were regarded as the reference dataset. This approach can accurately reveal the variation characteristics of the model

response due to parameter perturbation. Some studies have shown that sensitive parameters may vary when using different evaluation metrics (Tang et al., 2007; van Werkhoven et al., 2009). Hence, in this study, two common metrics, the TS and the RMSE, were used to evaluate the precipitation simulation results of the WRF model with perturbed parameter values. RMSE was also used to evaluate the temperature simulation results of the WRF model with perturbed parameter values. Precipitation evaluation functions were used to compute the simulation metrics (TS and RMSE) of 6-hourly and 24-hourly accumulated precipitation for the nine rainy events, and the temperature evaluation functions evaluated the simulation errors (RMSE) of 3-hourly average, 24-hourly average, 24-hourly maximum, and 24-hourly minimum temperature for the nine sunny events. Different model evaluation functions were used to conduct various parametric SA experiments, which helped to obtain more comprehensive parametric SA results.

The definitions of the TS can be stated as follows:

$$TS = \frac{NA}{NA + NB + NC}, \quad (1)$$

where, TS ranges from zero (poor) to one (good) and NA is the number of grid cells for which the simulated precipitation amounts with perturbed and default parameter values simultaneously satisfy the prescribed threshold interval. The different intervals represent different precipitation intensities, and the intensity ranks for 6-hourly and 24-hourly accumulated precipitation are given in Table 2. NB is the number of grid cells for which the simulated precipitation amount with the perturbed parameter values satisfies the prescribed threshold interval, but that with the default parameter values fails. NC is the number of grid cells for which the simulated precipitation amount with the default parameter values successfully satisfies the threshold interval, but that with the perturbed parameter values fails.

RMSE can be expressed as follows:

$$RMSE = \sqrt{\frac{\sum_{t=1}^T \sum_{i=1}^M (Sim_i^t - Def_i^t)^2}{MT}}, \quad (2)$$

where, Sim_i^t and Def_i^t represent the simulated results with perturbed and default parameter values at the i th grid cell and

at time t , respectively, and M and T are the total number of grid cells and time steps, respectively.

2.5 SA methods

To obtain more comprehensive information on the parametric sensitivity of precipitation and temperature in the WRF model, multi-uncertainty quantification methods, including three qualitative SA methods and one quantitative SA method based on a response surface model, were used to conduct parametric SA experiments on precipitation and temperature. These methods are briefly described in the following sections.

2.5.1 Qualitative SA methods

(1) Delta test. The delta test (DT) is an SA method based on residual noise variance estimation. In a regression equation, assuming M input points $(x_i)_{i=1}^M$ and associated scalar outputs $(y_i)_{i=1}^M$ with an additive noise term:

$$y_i = f(x_i) + \varepsilon_i, \quad i = 1, 2, \dots, M, \quad (3)$$

where the function f is assumed to be smooth and the residual noise $(\varepsilon_i)_{i=1}^M$ is independently and identically distributed with a mean of zero. The variance of the noise $(\varepsilon_i)_{i=1}^M$ can be estimated as:

$$Var(\varepsilon) \approx \frac{1}{2M} \sum_{i=1}^M (y_i - y_{N_s(i)})^2, \quad (4)$$

where, $N_s(i) = \arg \min_{k \neq i} \|x_i - x_k\|_S^2$ represents the nearest neighbor of the input point x_i in subset S , which is one of the variable subsets (total $2^q - 1$ subsets, where q is the dimensionality of all variables), and the right-hand term of eq. (4) is called the DT metric, $\delta(S)$, and represents the degree of fit of function f with subset S . If $\delta(S)$ is the minimum value in all the variable subsets of $2^q - 1$ DT metrics, then the input variables (or parameters) constituting S are the most sensitive parameters (Eiroola et al., 2008). The sensitivity score for parameter x_i ($i=1, 2, \dots, q$) is the ratio of the sum of DT metrics, including x_i , to the sum of all DT metrics in the first 50 minimum DT metrics.

(2) Sum of trees. The sum of trees (SOT) method is a tree-based regression method. It builds a regression model by recursively partitioning the data space and fitting a uniform function in each subspace (Breiman et al., 1984). If the partition in each parameter space causes a maximum decrease in the residual sum of squares, a split occurs. The splitting process does not terminate until the fitness error in each subspace is less than a prescribed threshold. The number of splits (NS) in each parameter space represents the sensitivity of the parameter, meaning that the greater the value of NS for a parameter, the more sensitive the parameter is. The sensitivity score for each parameter is the ratio of its NS to the maximum value of all parametric NS sets.

(3) Multivariate adaptive regression splines. The multivariate adaptive regression splines (MARS) method (Friedman,

Table 2 Precipitation intensity classification criteria

Precipitation rank	6-hour precipitation amount (mm)	24-hour precipitation amount (mm)
Light rain	[0.1, 4.0)	[0.1, 10.0)
Moderate rain	[4.0, 13.0)	[10.0, 25.0)
Heavy rain	[13.0, 25.0)	[25.0, 50.0)
Storm	[25.0, 60.0)	[50.0, 100.0)
Heavy storm	[60.0, 150.0)	[100.0, 250.0)
Severe storm	[150.0, 350.0)	[250.0, 450.0)

1991; Shahsavani et al., 2010) is an extension of SOT. Compared with SOT, MARS performs the same recursive partitioning of the parameter space, but uses a regression function in each subspace (e.g., a uniform function in SOT and a low-order function in MARS). In each subspace, the low-order function is built using basis functions that exist in three forms: a constant, a hinge function, and the product of several hinge functions. The linear combination of all basis functions forms a total regression function for the whole parameter space. Hence, the MARS method can construct a continuous regression model that provides a better fit than SOT. MARS uses two steps to construct a reasonable regression model: the forward step produces an overfitted model using paired hinge functions related to the input parameters, and the backward step prunes the overfitted model to the best model by repeatedly deleting the least effective term. After a suitable regression model M has been constructed, a generalized cross-validation (GCV) index is used to evaluate the model:

$$\text{GCV}(M) = \frac{1}{N} \frac{\sum_{i=1}^N (Y_i - \hat{Y}_i)^2}{\left[1 - \frac{1 + c(M)d}{N}\right]^2}, \quad (5)$$

where, N is the number of all data points before regression, Y_i is a data point, \hat{Y}_i is the estimated value of Y_i based on regression model M , d is the effective number of degrees of freedom, and $c(M)$ is a penalty factor for adding a low-order function. A lower GCV represents a better-fitting model.

Under a suitable regression model, the absolute increment of GCV with the removal of one parameter is an important parameter sensitivity metric (Steinberg et al., 1999). The larger the absolute increment of GCV when one parameter is removed, the more important that parameter is. The sensitivity score of the i th ($i=1, 2, \dots, n$) parameter is defined as:

$$\text{score}(i) = \frac{\Delta g(i)}{\max\{\Delta g(1), \Delta g(2), \dots, \Delta g(n)\}} \times 100, \quad (6)$$

where, $\Delta g(i)$ is the absolute increment of $\text{GCV}(M)$ when the i th parameter is removed.

2.5.2 Quantitative SA method

A qualitative SA method can provide the sensitivity ranks of parameters using fewer samples, but the parameter sensitivity scores are inaccurate due to the lack of a precise mathematical derivation. The quantitative SA method divides the total variance of the model response into the contribution of each parameter based on variance decomposition theory. As a quantitative SA method, the Sobol' method (Sobol', 1993, 2001) quantifies the attribution of the model response variance to specific-order terms of each parameter, providing a relatively accurate contribution ratio not only of the main effects of individual parameters, but also of the parameter interactions.

For the function $f(x_1, x_2, \dots, x_n)$ related to parameter x_i ($i=1,$

$2, \dots, n$), the corresponding variance decomposition equation can be expressed as:

$$V = \sum_{i=1}^n V_i + \sum_{1 \leq i < j \leq n} V_{i,j} + \dots + V_{1,2,\dots,n}, \quad (7)$$

where, V is the total variance of the function $f(x_1, x_2, \dots, x_n)$, V_i is the variance of the sub-function related to the i th parameter only, $V_{i,j}$ is the variance of the sub-function related to the i th and j th parameters only, and $V_{1,2,\dots,n}$ is the variance of the sub-function related to all parameters.

Normalizing to eq. (7) by dividing by V

$$\sum_{i=1}^n S_i + \sum_{1 \leq i < j \leq n} S_{i,j} + \dots + S_{1,2,\dots,n} = 1. \quad (8)$$

In the Sobol' method, the index S_i is referred to as the main effect (or first-order effect) of the i th parameter, and the index $S_{i,j}$ is referred to as the two-way interactive effect (or second-order effect) between the i th and j th variables. Another important index for the i th parameter is the total effect, which can be computed by summing the main effect of the i th parameter and all the interactive effects related to the i th parameter (Sobol', 2001).

As a quantitative SA method, the Sobol' method can obtain more reliable SA results than qualitative methods. However, Saltelli et al. (2000) found that a large number of samples (approximately 10^4 to 10^5) were required to compute reasonable Sobol' indices. Otherwise, the main effects and total effects significantly deviate from their analytical solutions, resulting in unreasonable SA conclusions. Obviously, it is completely intractable to perform approximately 10^5 runs of the WRF model with different parameter values. Hence, in this study, the Sobol' method was implemented on a simple statistical response surface model instead of the complex original model, avoiding tens of thousands of WRF model runs. In addition, the representativeness of the response surface model should be verified before conducting Sobol' analysis.

The relatively simple response surface model is not sufficient to estimate higher-order interactions, and therefore the higher-order interactive effects (>2) of the Sobol' method based on the response surface model are weak and negligible (Ziehn and Tomlin, 2009; Qian et al., 2015). Therefore, the total effect of a certain parameter is approximately equal to the sum of its main effect and all two-way interactive effects related to the parameter for the Sobol' method based on the response surface model. In this study, all response surface models were built using the MARS method (also called the MARS response surface model). In addition to the main and total effects of the individual parameters, the two-way interactions between the WRF parameters based on the MARS response surface model were also analyzed.

2.6 SA framework

An integral parametric SA experiment includes four major steps: (1) identifying the adjustable parameters of the model

and defining their ranges; (2) generating representative samples from the parameter space using a suitable sampling method; (3) running the model with different parameter samples and computing their output errors; and (4) assessing the parametric sensitivity using an SA method by combining the parametric sample values and the corresponding model output errors.

In this study, 18 parameters from six physical schemes of the WRF model were selected to conduct parametric SA experiments. Based on previous experience with sampling (Hou et al., 2012; Wang et al., 2014), a total number of samples equal to 10 times the parameter dimensionality can produce reasonable SA results using the QMC sampling method. Therefore, to use the simulation results of the WRF model effectively given its huge computation cost, 180 perturbed parameter values were included in the WRF model for the precipitation simulations of the nine rainy events and the temperature simulations of the nine sunny events. Compared with the simulation results of the WRF model with the default parameter values, the errors of the 180 WRF simulations with the perturbed parameter values were computed using the evaluation metrics (TS and RMSE for precipitation and RMSE for temperature). Based on the input parameter values and the corresponding model output errors, three qualitative SA methods (DT, SOT, and MARS) and one quantitative SA method (the MARS response surface model-based Sobol' method) were used to perform a systematic evaluation of the sensitivity of all 18 adjustable parameters to the precipitation and temperature simulation results of the WRF model.

The QMC sampling methods and the SA methods, including DT, SOT, MARS, and Sobol', were implemented using a software package called the Uncertainty Quantification Python Laboratory (UQ_PyL) (Wang et al., 2016). This software integrates many methods to build an efficient framework for uncertainty quantification (UQ). In the UQ framework, UQ_PyL provides design of experiments, statistical analysis, sensitivity analysis, surrogate modeling, and optimization.

3. Results

3.1 Parametric SA for precipitation simulation

3.1.1 Qualitative parameter screening

(1) Six-hourly accumulated precipitation. For comparison with the results of the corresponding precipitation simulations with default parameter values, the TS and RMSE of the 6-hourly accumulated precipitation simulations with the perturbed parameter values were computed for the nine rainy events. Then the qualitative SA method was applied to the combinations of all the perturbed parameter values and their

corresponding model output metrics (TS or RMSE). The TS metric was calculated as precipitation ranks. Six categories of precipitation were defined (light rain, moderate rain, heavy rain, storm, heavy storm, and severe storm) according to differences in precipitation amount (see Table 2). Based on sample size considerations, only the first four precipitation categories were analyzed. The sensitivity scores of all 18 adjustable parameters for the TS of 6-hourly accumulated precipitation (categorized as light rain, moderate rain, heavy rain, and storm) using three qualitative SA methods (DT, SOT, and MARS) are shown in Figures 3a–d. Another metric, RMSE, was also used to evaluate the simulation results of all 6-hourly accumulated precipitation amounts for the nine rainy events; the parametric sensitivity scores for RMSE of 6-hourly accumulated precipitation are shown in Figure 3e. In each subgraph of Figure 3, the horizontal axis denotes the 18 adjustable parameters of the WRF model, and the vertical axis denotes the sensitivity scores according to the three qualitative SA methods. The parameter sensitivity scores for each SA method were normalized to [0, 1], as shown in Figure 3. The score of the most sensitive parameter was 1, and the score of the most insensitive parameter was 0. Figures 3a–d show that four parameters (P5, P7, P10, and P16) were common sensitive parameters for all four precipitation categories. DT, SOT, and MARS produced consistent results for the sensitive parameters, but there were significant discrepancies in the results for the moderately sensitive parameters. For instance, the moderately sensitive parameters for TS of storm were P3, P9, and P17 using MARS, but P4 and P12 using DT. The moderately sensitive parameters were also inconsistent among the four precipitation categories. The sensitive parameters for RMSE were the same as those of TS for the four precipitation categories, a result that demonstrates that the sensitive parameters for 6-hourly accumulated precipitation do not vary with different evaluation metrics or qualitative SA methods.

(2) Twenty-four-hourly accumulated precipitation. The SA experiments for 24-hourly accumulated precipitation were designed in the same way as those for 6-hourly accumulated precipitation. The sensitivity scores of the parameters for TS and RMSE of 24-hourly accumulated precipitation are shown in Figure 4. The common sensitive parameters were P5, P7, P10, and P16, which is consistent with the results for 6-hourly accumulated precipitation. The conclusions regarding the screened sensitive parameters were also unaffected by the choice of SA method or evaluation metric.

3.1.2 Quantitative SA

Quantitative SA methods require a large number of samples to analyze parameter sensitivity, unlike qualitative methods that require fewer samples. Therefore, the results of quantitative methods are more reliable and can be used to validate

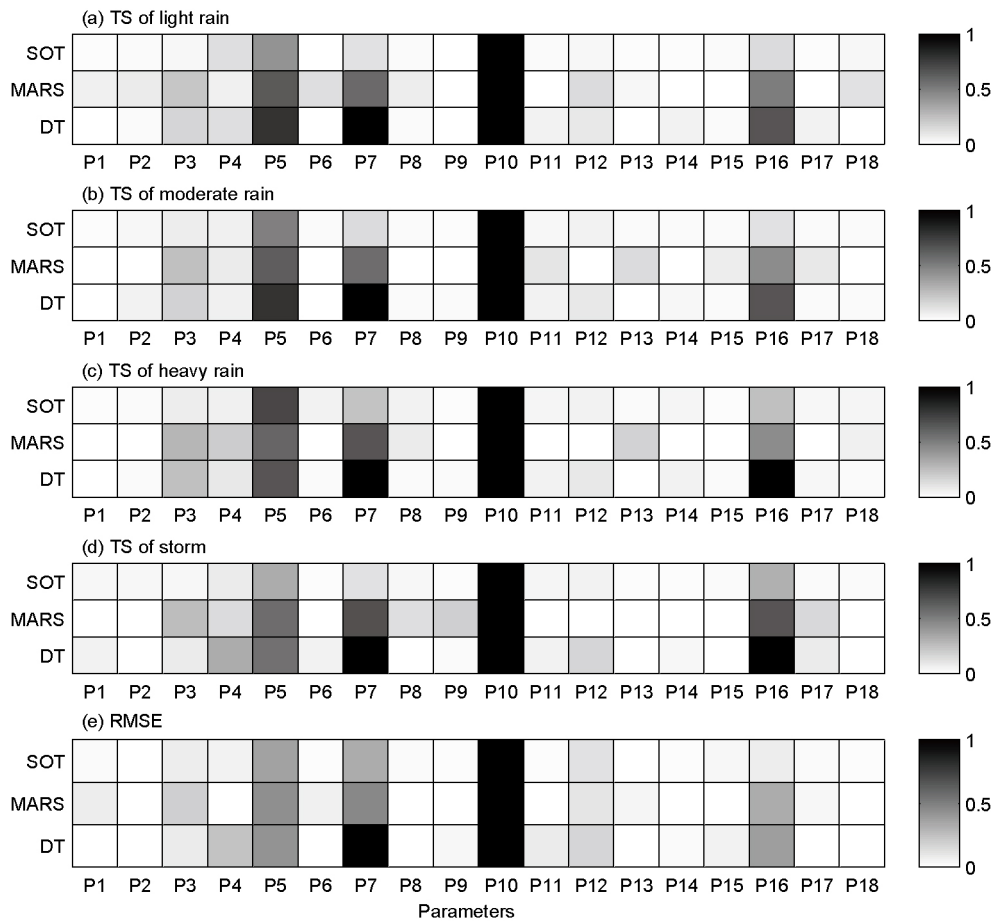


Figure 3 Parametric sensitivity scores of the three qualitative SA methods (DT, MARS, and SOT) for 6-hourly accumulated precipitation. The sensitivity scores are normalized to [0, 1]; 1 means most sensitive and 0 means least sensitive.

the results of qualitative methods. In addition, quantitative methods accurately produce not only sensitivity scores for individual parameters (by computing the contribution ratio of the main effect of each individual parameter to the total variance of the model response), but also the interaction effects among parameters. The large number of samples required for quantitative SA methods requires a correspondingly large number of model runs, which is impractical for the WRF model given its high computational cost. However, the statistical response surface model can be rapidly evaluated in several seconds, and therefore it is recommended to conduct quantitative SA analysis on a response surface model instead of the original physical model, provided that the two models have similar responses. In this study, the Sobol' method was applied to the MARS response surface model instead of the original WRF model to obtain the quantitative parametric SA analysis results.

(1) Evaluation of the MARS response surface model. The representativeness of the response surface model with respect to the original model is an important index to determine whether the SA results based on the response surface model are reliable. Therefore, the accuracy of the response surface model must be verified before the Sobol' method

is applied to it. The goodness of fit of the MARS response surface model to the response from the WRF model can be adjusted by controlling the number of hinge functions. Figure 5 shows scatter plots of the MARS-fitted TS (RMSE) values against the WRF-simulated TS (RMSE) values on 180 parametric samples for 6-hourly and 24-hourly accumulated precipitation. The MARS response surface models estimated the metrics of different precipitation output variables with R^2 varying from 0.824 for TS of 24-hourly accumulated heavy rain to 0.964 for TS of 24-hourly accumulated light rain.

(2) Main and total effects of individual parameters. Based on the MARS response surface models as constructed, the Sobol' method was used to conduct parametric quantitative SA for precipitation simulations using the WRF model. The sample size was 100000. The main and total effects of the 18 parameters for 6-hourly and 24-hourly accumulated precipitation simulations with the two metrics (TS and RMSE) are shown in Figure 6. In each subfigure, the black bar denotes the main effect (first-order sensitivity), and the white bar represents the interactive effect summing all two-way interactive effects related to the specific parameter. The total effect of a parameter is the sum of its main effect and its interactive effect. The interactive effects of P7 and P10 are also evident,

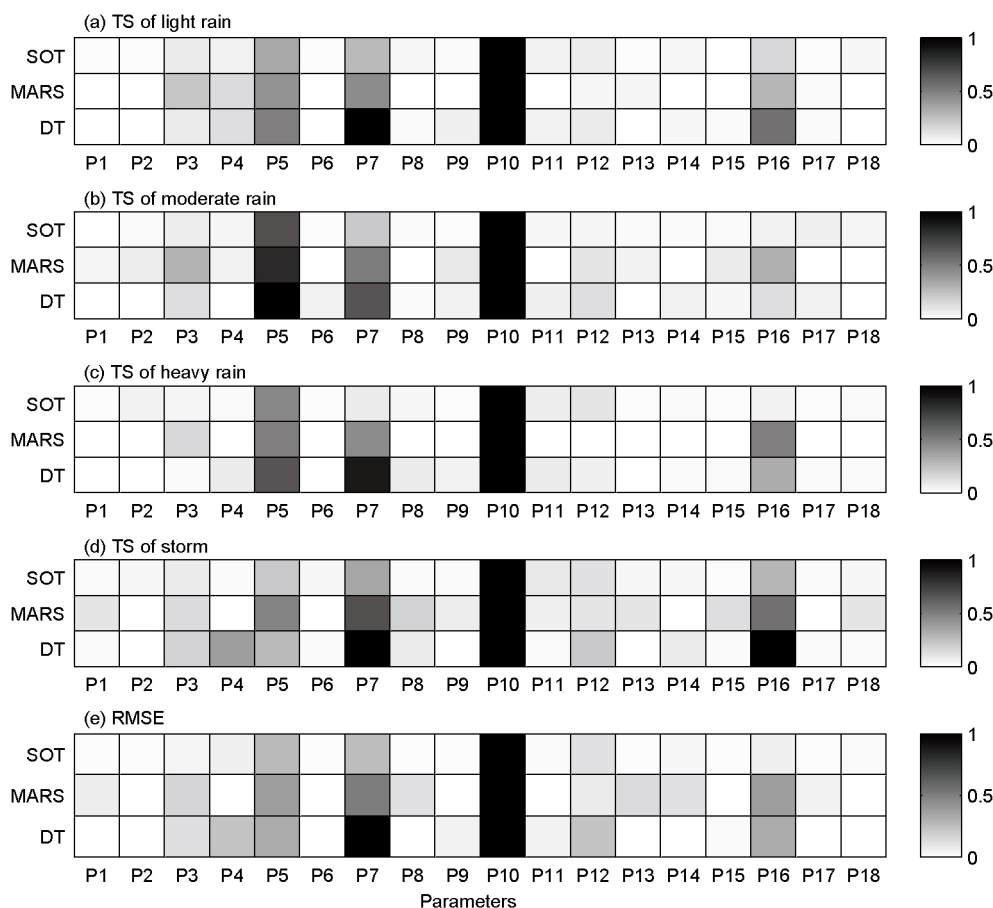


Figure 4 Parametric normalized sensitivity scores of the three qualitative SA methods (DT, MARS, and SOT) for 24-hourly accumulated precipitation.

which means that the response relationship between the model precipitation errors and the input parameter values is nonlinear.

Overall, five parameters were sufficient to explain the variance of the model response for 6-hourly and 24-hourly accumulated precipitation based on the SA results for the main and total effects of individual parameters. In agreement with the parametric screening results of the qualitative SA methods (see Figures 3 and 4), the four main sensitive parameters for 6-hourly and 24-hourly accumulated precipitation were P5, P7, P10, and P16, and the most sensitive parameter was P10. Note that P3 followed the four main sensitive parameters for all output-evaluated precipitation functions according to the total effect ranks of the 18 parameters, a result that differed from the case of qualitative SA. Based on qualitative and quantitative SA results, the five most sensitive parameters for precipitation were identified as P3, P5, P7, P10, and P16. In addition to screening results for sensitive parameters, the quantitative SA method also provides the two-way interactive effects between parameters. In Figure 6, all two-way interactive effects related to a certain specific parameter are summed as the total interactive effect of each parameter. Figure 6 shows that the parametric interaction effect arose mainly from P7 and P10, whereas more parameters provided an inter-

active effect in the storm rankings. This may have been due to more complex storm mechanisms or fewer storm samples.

(3) Quantifying the relative contribution ratios of individual parameters. According to the definition of the parametric total effect in eq. (8), the sum of all parametric total effects is greater than one. Therefore, the relative contribution of each individual parameter to the total variance of the model response is defined by the ratio of its total effect to the sum of all parametric total effects. The relative contribution ratios of the individual parameters with the top six ranks are shown in Figure 7. P10 plays the most significant role in the contribution to model response variance for 6-hourly and 24-hourly accumulated precipitation simulations using the two metrics (TS and RMSE). P5, P7, P16, and P3 followed P10 as common important parameters, but their rankings varied when different precipitation evaluation functions were used. The parameters ranked sixth were inconsistent. For instance, P4 was the sixth most important parameter for moderate rain and heavy rain in the case of 6-hourly accumulated precipitation and for light rain in the case of 24-hourly accumulated precipitation. P6 was the sixth most important parameter when considering the RMSE of 6-hourly accumulated precipitation and heavy rain in the case of 24-hourly accumulated precipitation. P12 was the sixth most important parameter for light

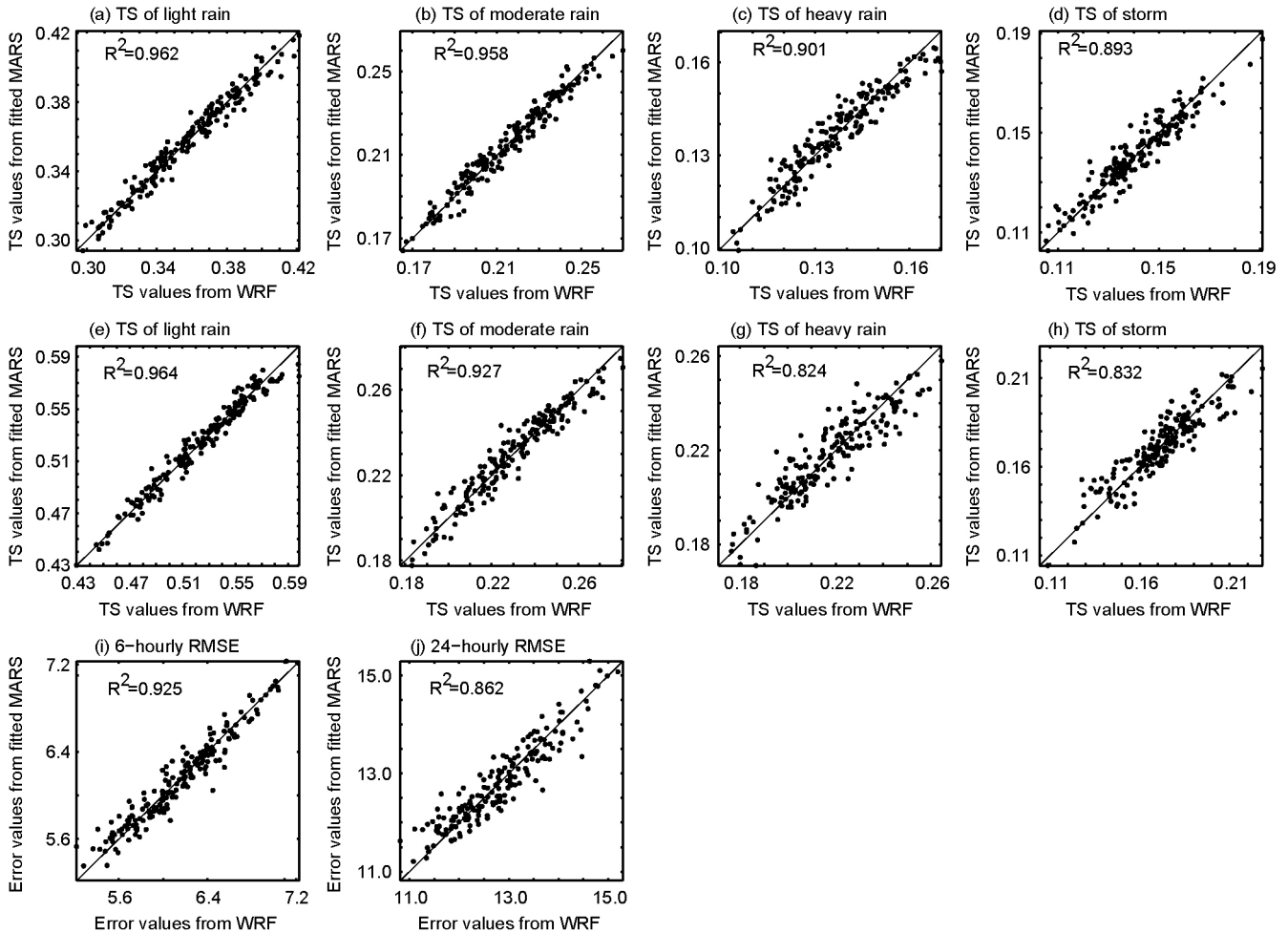


Figure 5 Scatter plots of MARS-fitted precipitation errors against WRF-simulated precipitation errors for (a)–(d) TS of 6-hourly accumulated precipitation, (e)–(h) TS of 24-hourly accumulated precipitation, and (i)–(j) RMSE of 6-hourly and 24-hourly accumulated precipitation.

rain in the case of 6-hourly accumulated precipitation and for moderate rain in the case of 24-hourly accumulated precipitation. P9, P15, and P8 were the sixth most important parameter for storm in the case of 6-hourly accumulated precipitation and for storm and for RMSE of 24-hourly accumulated precipitation, respectively. Overall, the contributions of the first five parameters to the total variance of the model response for 6-hourly and 24-hourly precipitation varied from 90.48% for light rain in the case of 6-hourly accumulated precipitation to 99.99% for heavy rain in the case of 24-hourly accumulated precipitation. The one exception was a contribution of 75.23% for storm in the case of 24-hourly accumulated precipitation. Therefore, it is feasible and highly efficient to conduct parameter optimization for precipitation simulation using the WRF model by adjusting these five parameters while keeping the other parameters fixed at their default values.

(4) Quantifying the contribution ratios of the main effects of individual parameters and the two-way interactive effects between parameters. To quantify the effect of parameter interactions accurately, the contribution ratios of the main effects of individual parameters and the two-way interactive ef-

fects between parameters to the total variance of the model response were computed for each precipitation output variable based on 100000 samples from a suitable MARS response surface model. Figures 8 and 9 show the contribution percentages of the parametric effects (main effects of the individual parameters and their two-way interactive effects) to the total variance of 6-hourly and 24-hourly accumulated precipitation metrics. The main contributions to total variance were derived from the main effects of individual sensitive parameters and the two-way interactive effect between P7 and P10. Overall, the accumulated contribution percentages of the main effects of individual sensitive parameters (P3, P5, P7, P10, and P16) varied from 57% for heavy rain to 76% for moderate rain for 6-hourly accumulated precipitation, and from 65% for RMSE to 84% for heavy rain for 24-hourly accumulated precipitation, except for 45% for storm. The contribution percentages of the main effect of the most sensitive parameter, P10, for light rain, moderate rain, heavy rain, storm, and RMSE for 6-hourly (24-hourly) accumulated precipitation were 28.42% (50.27%), 41.26% (36.85%), 25.41% (47.35%), 26.48% (13.96%), and 35.53% (38.63%), respec-

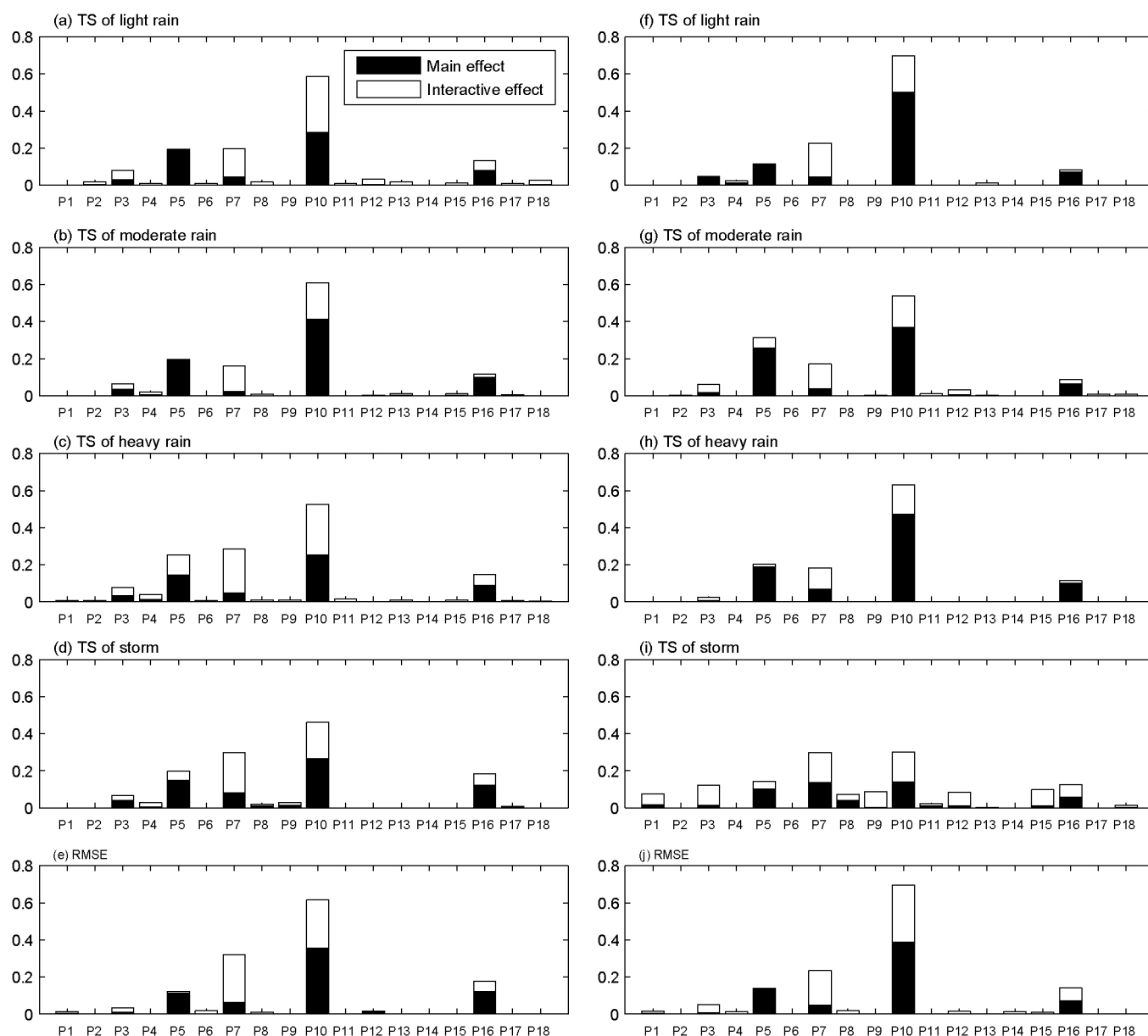


Figure 6 Sobol' SA indices of individual parameters for ((a)–(e)) 6-hourly and ((f)–(j)) 24-hourly accumulated precipitation simulations with two metrics (TS and RMSE).

tively. The accumulated contribution percentages of the main effects of the individual sensitive parameters in the case of 24-hourly accumulated precipitation were higher than those from 6-hourly accumulated precipitation. This effect arose because the impact of the parameters on the simulation results was more evident when the simulation integration time was longer. In addition to the main effect of each individual sensitive parameter, the contribution of the two-way interactive effect between P7 and P10 was also evident, varying from 12.69% for light rain to 20.45% for RMSE for 6-hourly accumulated precipitation and from 9.25% for storm to 18.66% for RMSE for 24-hourly accumulated precipitation. Overall, the range of the accumulated contribution ratios for the main

effects of the five individual sensitive parameters and one interactive effect between P7 and P10 varied from 76% for light rain to 90% for moderate rain for 6-hourly accumulated precipitation and from 84% for RMSE to 95.2% for heavy rain for 24-hourly accumulated precipitation, except for 54% for storm.

3.2 Parametric SA for temperature simulation

3.2.1 Qualitative parameter screening

For comparison with the results of the corresponding temperature simulations using the WRF model with default param-

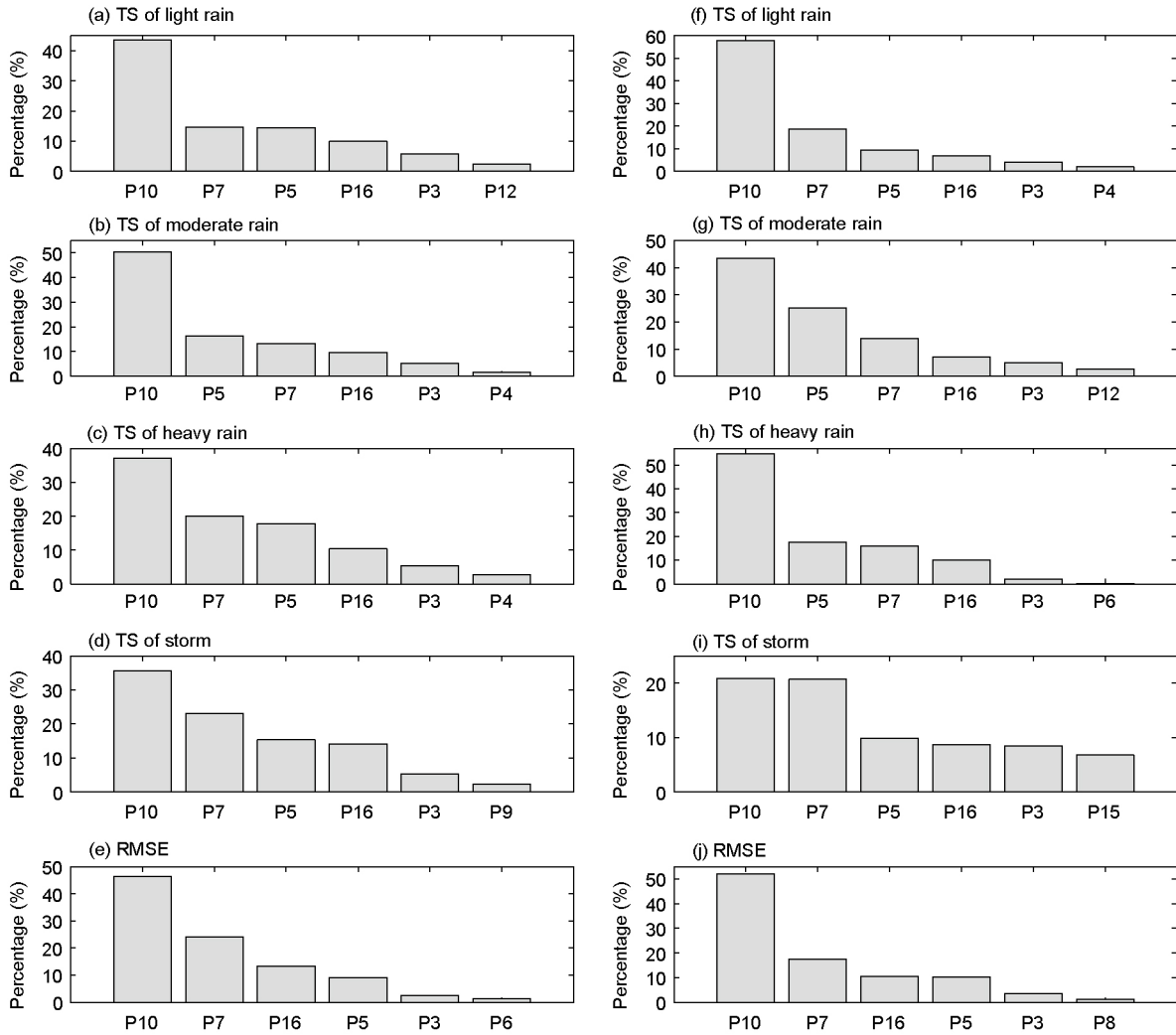


Figure 7 Relative contribution percentages of the top six sensitive parameters to the total effects of individual parameters for 6-hourly ((a)–(e)) and 24-hourly ((f)–(j)) accumulated precipitation simulations with two metrics (TS and RMSE).

eter values, the RMSE values of the 3-hourly average, 24-hourly average, 24-hourly maximum, and 24-hourly minimum temperature simulations using the WRF model with perturbed parameter values for the nine sunny events were computed. Qualitative SA was performed on the combinations of all perturbed parameter values and their corresponding temperature simulation errors (RMSE). The normalized SA scores of the parameters using the three qualitative SA methods (DT, MARS, and SOT) are shown in Figure 10. The most sensitive score is 1, and the most insensitive score is 0. From Figure 10, the common sensitive parameters for 3-hourly average, 24-hourly average, 24-hourly maximum, and 24-hourly minimum temperature simulations using the RMSE metric were found to be P7 and P10. The number of sensitive parameters was less than for precipitation. The two sensitive parameters for temperature were also identified as sensitive for precipitation, and P10 was the most sensitive parameter for both precipitation and temperature.

3.2.2 *Quantitative SA*

The Sobol’ method was then applied to the MARS response surface model instead of the WRF model. The response surface model was built by the MARS method with 180 sample points. The response surface model was fitted to the original WRF response by adjusting the number of hinge functions, and suitable MARS response surface models were identified for different output evaluation functions. The corresponding MARS response surface models evaluated the response for 3-hourly average, 24-hourly average, 24-hourly maximum, and 24-hourly minimum temperature on 180 parameter sets, obtaining R^2 values of 0.993, 0.991, 0.992, and 0.997, respectively (Figures not shown).

Quantitative SA experiments were then conducted on the most reasonable MARS response surface model using the Sobol’ method with 100000 samples. Figure 11 shows the main and total effects of the 18 parameters for the 3-hourly average, 24-hourly average, 24-hourly maximum, and 24-hourly minimum temperature simulations using the

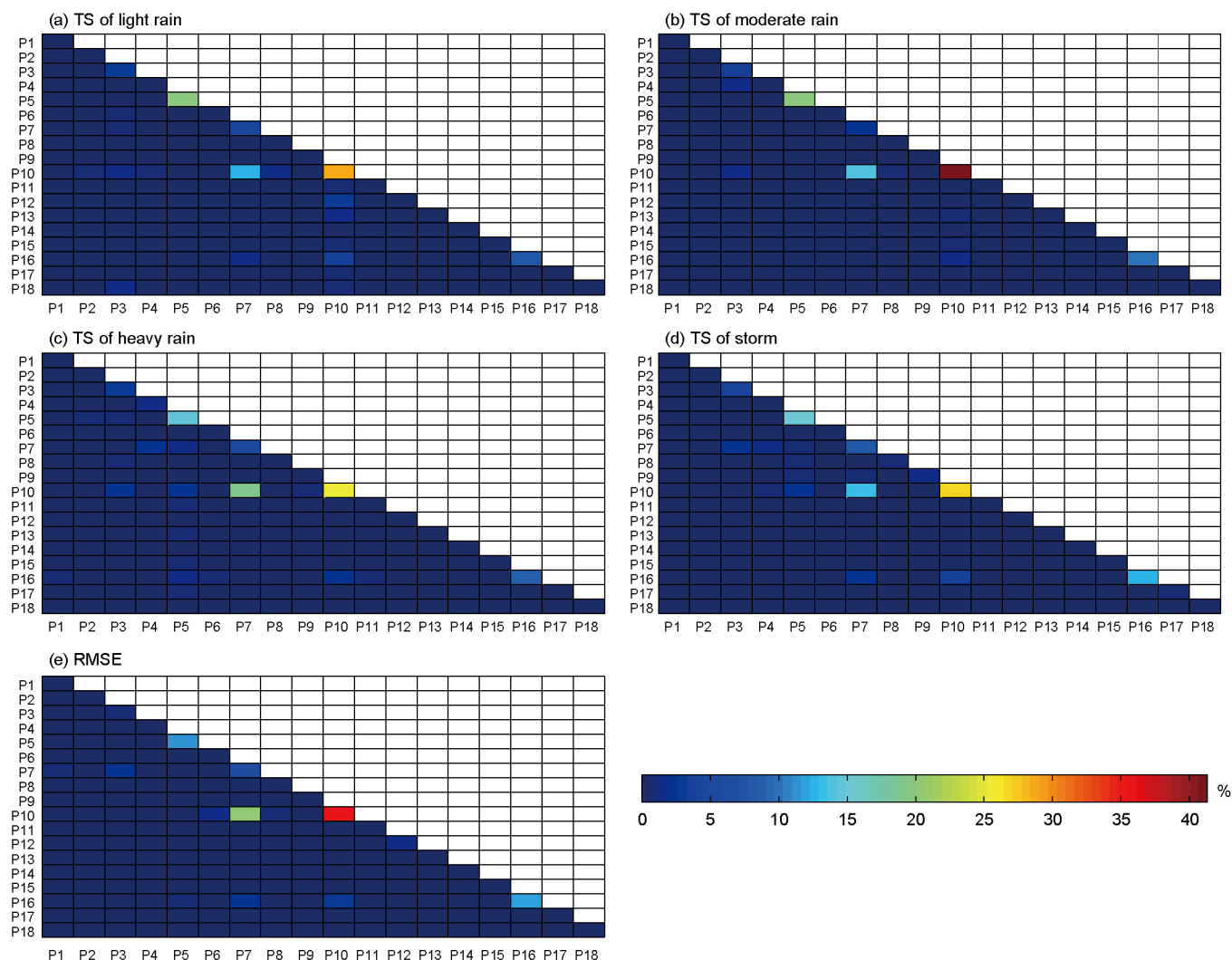


Figure 8 Contribution percentages of the main effects of individual parameters and two-way interactive effects between parameters to the total variance of 6-hourly accumulated precipitation simulations with two metrics (TS and RMSE).

RMSE metric. In each subfigure, the black and white bars represent the main effect (first-order sensitivity) and the interactive effect respectively. The definitions of interactive and total effects are the same as in the quantitative SA experiments for precipitation. According to the rankings of parametric total effects (or main effects), the most sensitive parameters were P7 and P10, a result that is consistent with the conclusions of qualitative parameter screening for temperature (see Figure 10). The interactive effect for temperature was found mainly between parameters P7 and P10 for 24-hourly average and maximum temperature; P10 has more interactive effects with other parameters than P7 for 3-hourly average and 24-hourly minimum temperature. Except for 24-hourly maximum temperature, the interactive effects between parameters P7 and P10 for temperature were weaker than for precipitation. The relative contribution ratios of the individual parameters (i.e., their percentages of the total parametric effects) for temperature were also computed. The relative contribution ratios of P7 (P10) to the total effect for

3-hourly average, 24-hourly average, 24-hourly maximum, and 24-hourly minimum temperature were 10.9% (82.2%), 42.6% (40.1%), 21.0% (68.2%), and 5.7% (85.3%), respectively. The sum of the total effects of P7 and P10 contributed more than 82% of the total variance of the temperature response, ranging from 82.7% for 24-hourly average temperature to 93.1% for 3-hourly average temperature.

To quantify the interactive effects of the temperature parameters accurately, the contribution ratios of the main effects of the individual parameters and of the two-way interactive effects between the parameters to the total variance of the model response were computed for each temperature output variable, based on 100000 samples from a suitable MARS response surface model. Overall, the accumulated contributions of the main effects of the individual sensitive parameters (P7 and P10) for 3-hourly average, 24-hourly average, 24-hourly maximum, and 24-hourly minimum temperature were 93%, 73%, 55%, and 89%, respectively. For 24-hourly average and 24-hourly maximum temperature, the highest

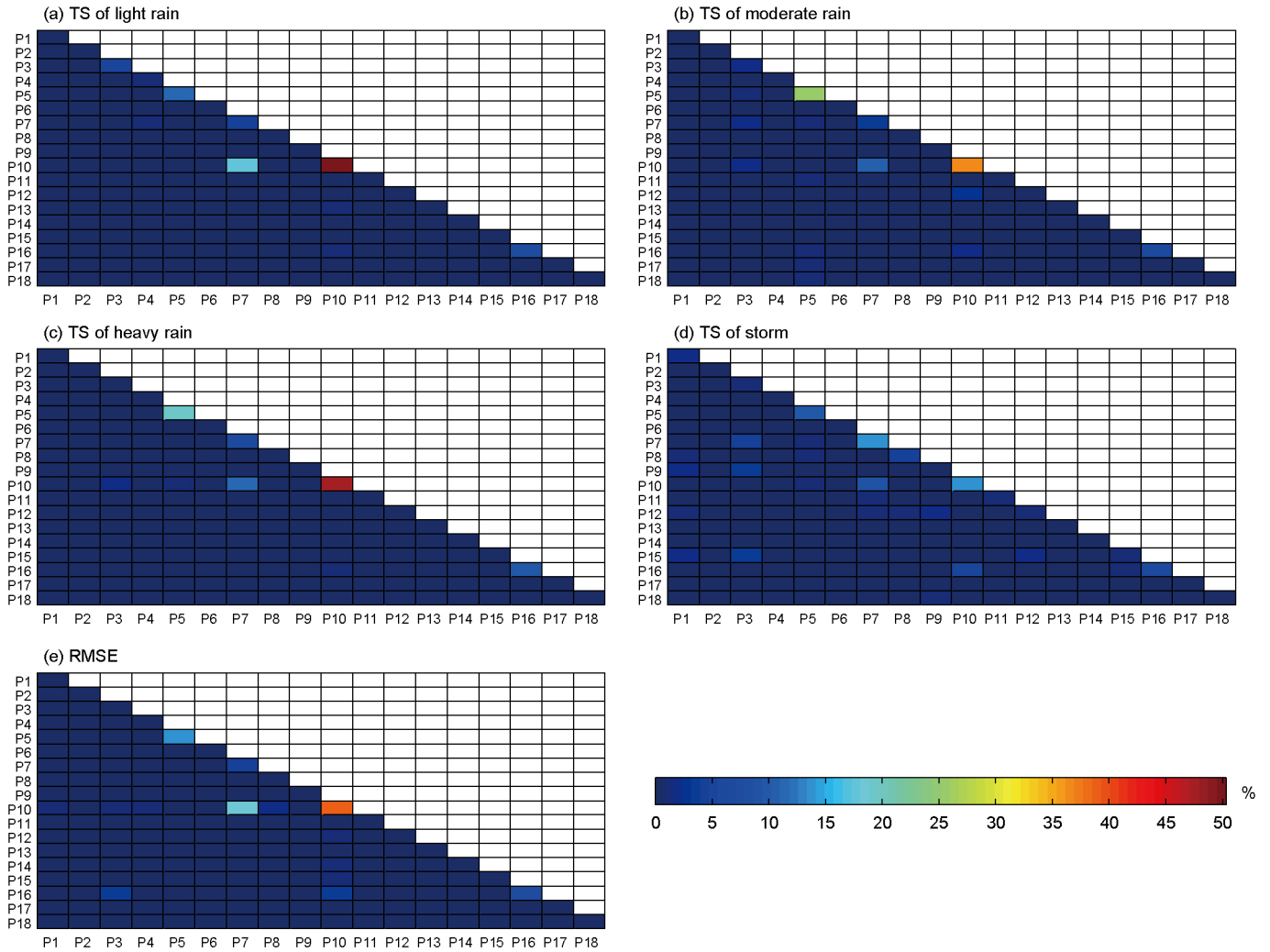


Figure 9 Contribution percentages of the main effects of individual parameters and two-way interactive effects between parameters to the total variance of 24-hourly accumulated precipitation simulations with two metrics (TS and RMSE).

contribution ratio among the two-way interactive effects occurred for the two-way interactive effect between parameters P7 and P10, at 5.3% and 29%, respectively. The total contribution ratios of all two-way interactive effects between parameters were less than 2% for 3-hourly average and 24-hourly minimum temperature (Figures not shown). Therefore, except for 24-hourly maximum temperature, the interactive effects between parameters for temperature were weaker than for precipitation.

3.3 Response of WRF output errors to sensitive parameters

To carry out a preliminary exploration of the optimal values of the sensitive parameters, observed precipitation and temperature data were chosen to evaluate the errors in the WRF precipitation and temperature simulations from the previous qualitative SA experiments. The observed precipitation data came from the China Hourly Merged Precipitation Analysis (CMPA-Hourly) product, with a horizontal spatial resolution

of 0.1° in latitude and longitude and a temporal resolution of one hour (Shen et al., 2014). The temperature-gridded data came from the land-surface forcing-field products for the Chinese mainland (Huang et al., 2014). Out of consideration for simulation accuracy, only the 6-hourly accumulated precipitation simulations with the TS metric and the 3-hourly average temperature simulations with the RMSE metric were analyzed in this study.

3.3.1 Response of precipitation errors to the five sensitive parameters

A uniform index was used to evaluate the four categories of simulated precipitation with different TS ranges. The normalized TS metric can be expressed as follows:

$$F(\theta) = -\frac{1}{4} \sum_{j=1}^4 \frac{f_j(\theta)}{f_j(\theta_{\text{def}})}, \quad (9)$$

where $f_j(\theta)$ is the TS value of simulated precipitation with perturbed parameter θ for the j th type of precipitation compared

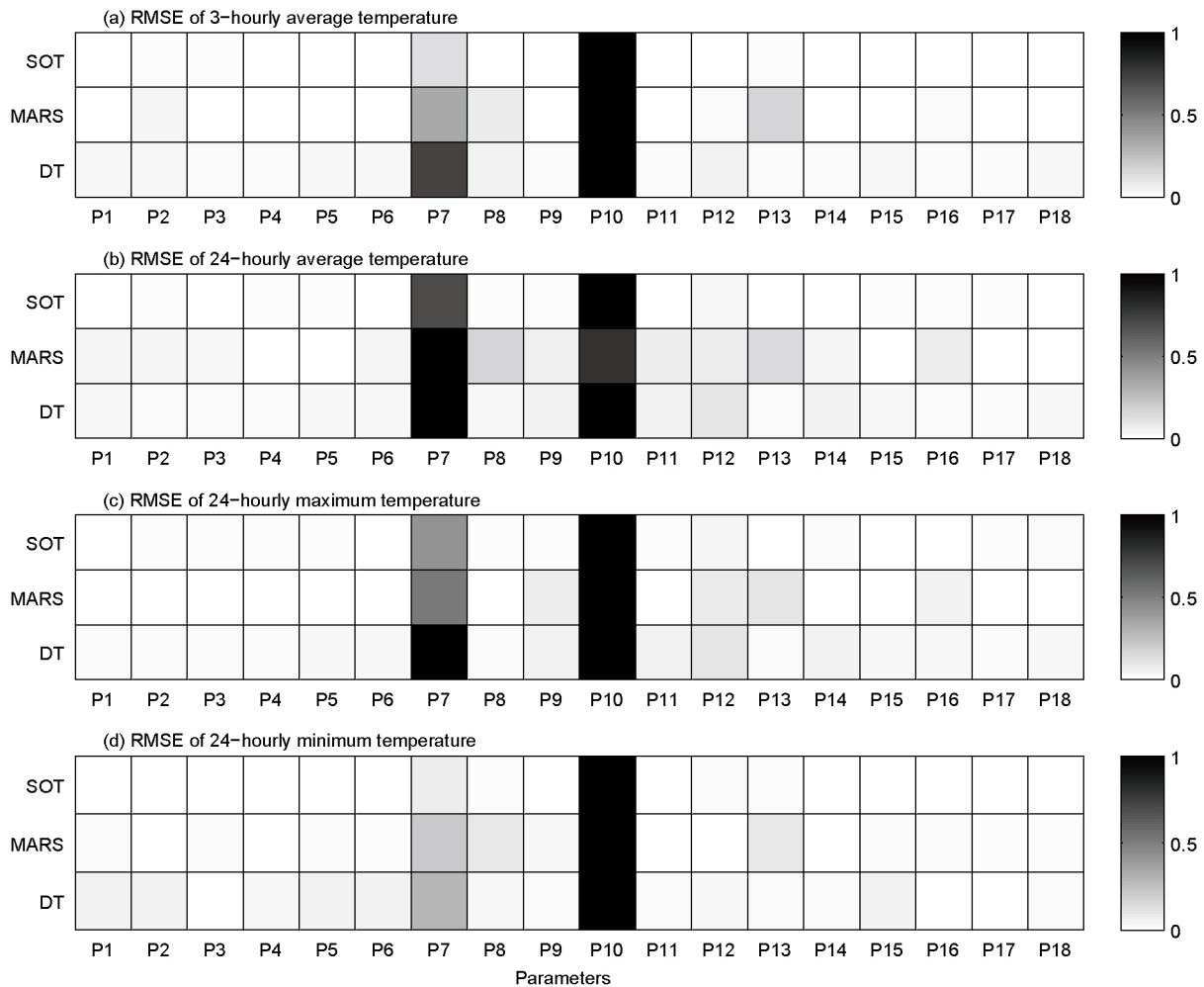


Figure 10 Parametric sensitivity scores of the three qualitative SA methods (DT, MARS, and SOT) for 3-hourly average, 24-hourly average, 24-hourly maximum, and 24-hourly minimum temperature. The sensitivity scores are normalized to [0, 1]; 1 means most sensitive, and 0 means least sensitive.

with the corresponding observed data; j is equal to 1, 2, 3, or 4, representing light rain, moderate rain, heavy rain, and storm, respectively; and (θ_{def}) represents the default parameter values. The negative sign ensures that better simulation results have smaller normalized TS.

Using the normalized TS index, 180 simulation results for 6-hourly accumulated precipitation from the previous qualitative SA experiments were used to analyze the response of the WRF precipitation simulation to its five sensitive parameters. The results are shown in Figure 12. In each sub-figure, the black cross indicates the simulation error of the WRF model with the default parameter values, and the curved line represents the average of 180 simulation results grouped into 20 bins (each bin including nine simulation results) for each input parameter. Simulated precipitation was more sensitive to P10 (*porsl*), P7 (*cssca*), and P5 (*dimax*) than to P3 (*ice_stokes_fac*) and P16 (*pfac*), a result that is consistent with the conclusions of the previous parametric SA experiments. Compared with the respective optimal parameter values, the default values of P3 and P5 were lower, and the de-

fault values of P7, P10, and P16 were higher. Most of the normalized TS values for the five sensitive parameters were lower than the normalized TS values of the default parameters, an observation that demonstrates the potential to improve WRF precipitation simulation results by adjusting the five sensitive parameter values.

3.3.2 Response of temperature errors to the two sensitive parameters

By dividing by the RMSE of the corresponding WRF simulations with default parameter values, all the RMSE values for 3-hourly average temperature simulation results in the previous 180 simulations used for qualitative SA of temperature were normalized. The response of the normalized RMSE errors to the sensitive parameters P7 (*cssca*) and P10 (*porsl*) is shown in Figure 13. The normalized RMSE error for the simulation results with the default parameter values was 1.0. The smaller the normalized RMSE error, the closer the simulated results are to the observations. Figure 13 shows that P10 had a greater impact on the model response variance than P7, a

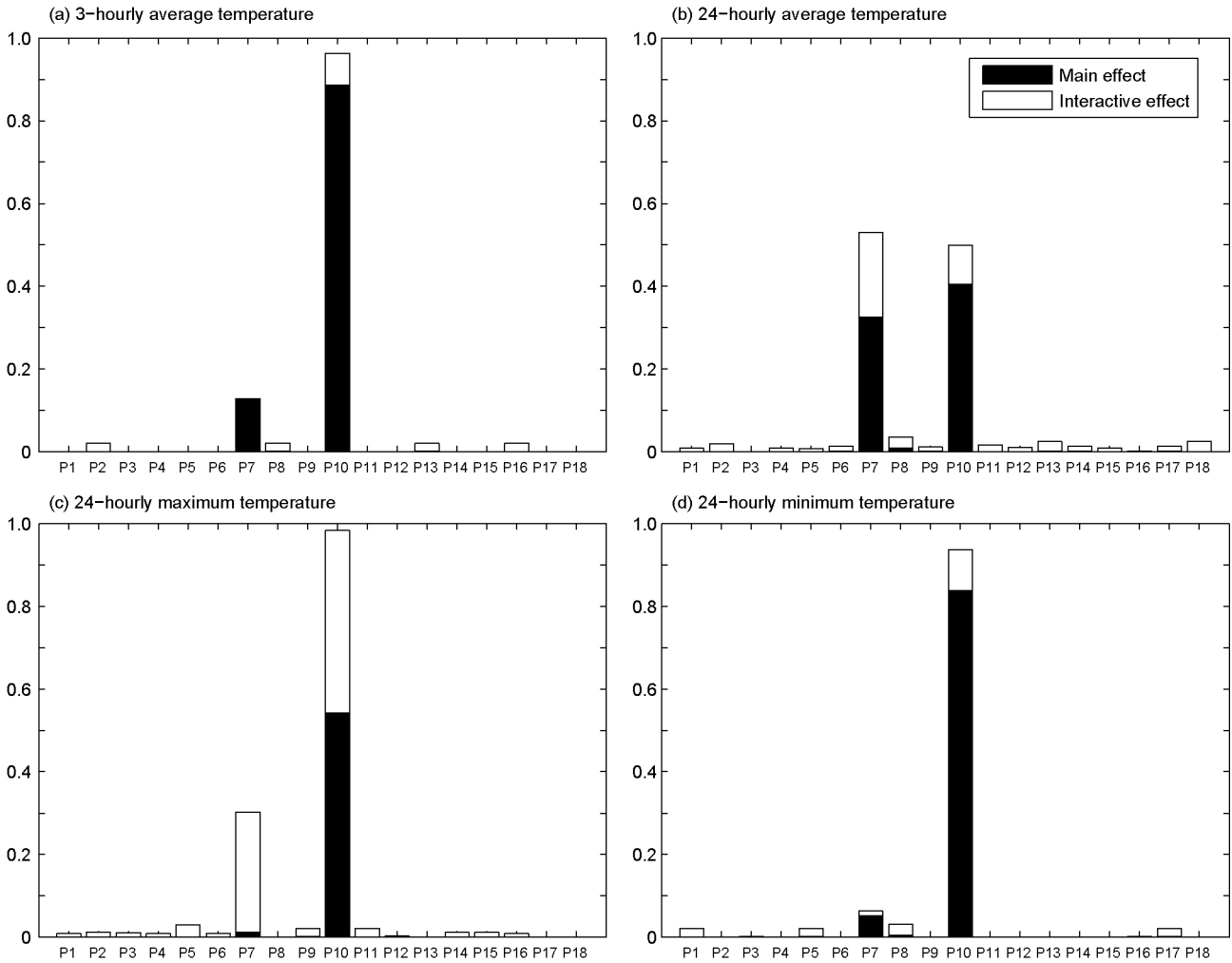


Figure 11 Sobol' SA indices of the individual parameters for 3-hourly average, 24-hourly average, 24-hourly maximum, and 24-hourly minimum temperature simulations with the RMSE metric.

result that is consistent with the parametric SA results for temperature. There were fewer points with RMSE values lower than the RMSE value of the default parameters, and therefore the lowest point on the average line is higher than the default parameter point (i.e., the black cross point). However, the default values of both P7 and P10 were higher than their optimal values according to the tendency of the average lines.

3.3.3 Improvement by parametric optimization

To examine the possibility of improving the WRF model by parameter optimization, the simulation results with the default parameter values were compared to the results with the optimal parameter values for 6-hourly accumulated precipitation and 3-hourly average temperature. The optimal simulation results for 6-hourly accumulated precipitation and 3-hourly average temperature were obtained by searching for the minimum normalized metric in the respective 180 simulations of the qualitative SA experiments. Table 3 shows the percentage improvements for 6-hourly accumulated precipitation and 3-hourly average temperature. The optimal

parameter values improved the simulation results for the four precipitation categories; in particular, the improvement ratios for moderate and heavy rain were 20% and 20.83%, respectively. The average percentage improvement in the four categories of 6-hourly accumulated precipitation was 12%. The simulation results for 3-hourly average temperature were improved by 8.52%.

Figure 14 shows the spatial differences between the default and optimal simulation results for precipitation and temperature. The left panel shows the spatial distribution of the observed daily average precipitation for the nine rainy events, the corresponding simulation residuals using the default parameter values, and those using the optimal parameter values. The same comparison for temperature is shown in the right panel of Figure 14. The optimal parameter values were found to improve the precipitation simulation results over the default parameter values, especially for stronger precipitation. Similarly, the improvement in the temperature simulation using the optimal parameter values was more evident in the south, with its higher temperature values. Although the pre-

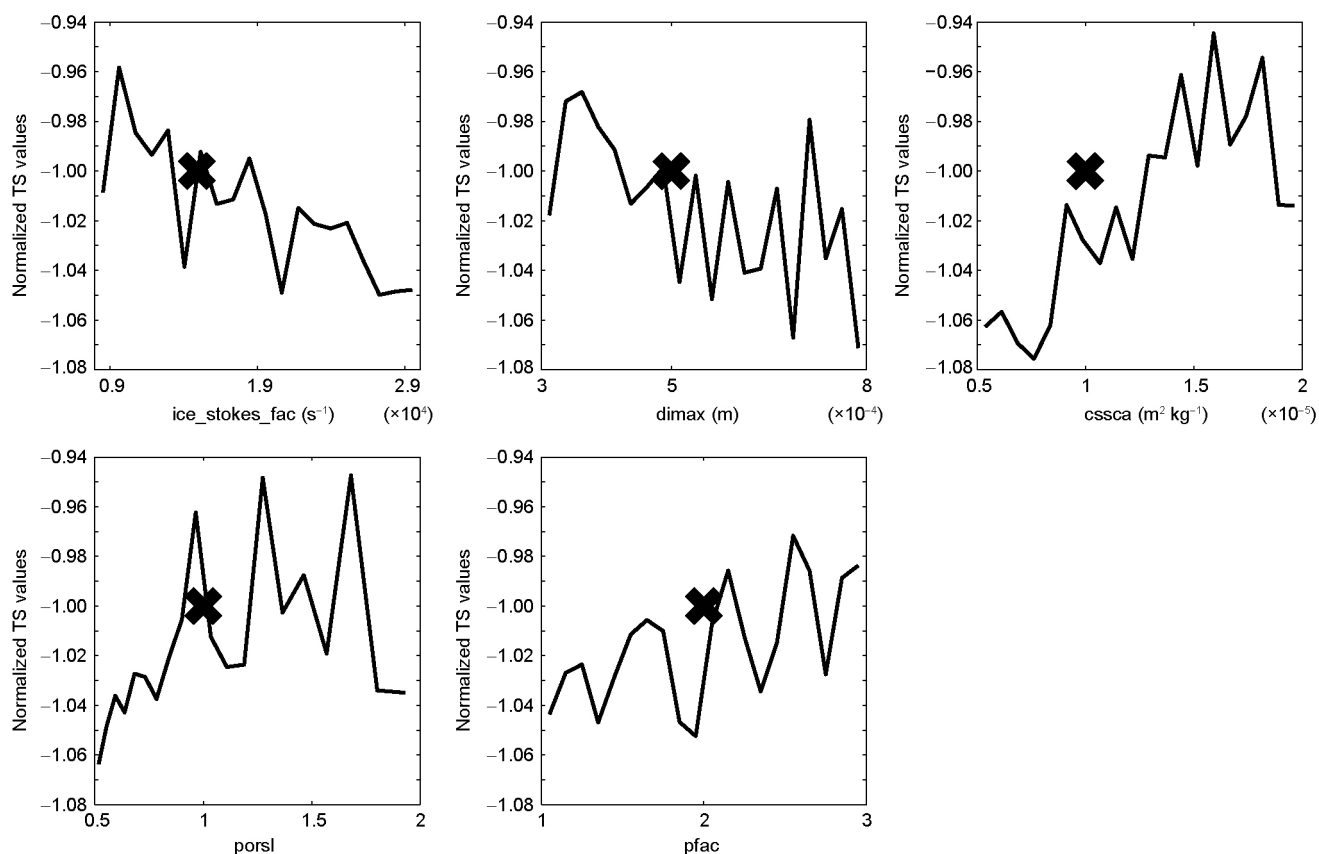


Figure 12 Response of 6-hourly accumulated precipitation to the five sensitive parameters in 180 simulations compared with observed data.

Table 3 Scores of precipitation and temperature simulations using default and optimized parameter sets

Metric	Name	Default	Optimized	Improvement
TS (6-hourly precipitation)	Light rain	0.165	0.169	2.42%
	Moderate rain	0.072	0.087	20.83%
	Heavy rain	0.035	0.042	20.00%
	Storm	0.041	0.043	4.88%
	Total	1.000	1.120	12%
RMSE (3-hourly average temperature (°C))	Temperature	1.408	1.288	8.52%

precipitation and temperature optimization results in Figure 14 were obtained by searching for the minimum simulation errors of the corresponding variables from their 180-parameter perturbation simulations for the qualitative parametric SA, they reflect the potential of their respective sensitive parameters to improve precipitation and temperature simulation results. This is the case because the sensitive parameters contribute most of the variance in model response based on the quantitative parametric SA results. If a more powerful optimization method were used to adjust the sensitive parameter values, greater improvement would be achieved.

3.4 Physical interpretation of the sensitive parameters

According to the previous parametric SA results, the sensitive parameters for precipitation were P3, P5, P7, P10, and

P16, and the sensitive parameters for temperature were P7 and P10. However, the physical meaning of the sensitive parameters should be discussed to determine how they affect the precipitation and temperature simulation results. For the microphysics scheme, P3 (scaling factor applied to ice fall velocity) and P5 (limiting maximum value for cloud-ice diameter) have similar effects on precipitation because they jointly affect the conversion from cloud ice to rain water. P7 (scattering tuning parameter) from the shortwave scheme directly influences the amount of downward solar radiation reaching the ground and hence the amount of water vapor that evaporates from the surface, bringing about changes in temperature and precipitation. P10 (multiplier for the saturated soil water content) from the Noah land-surface scheme directly affects water and heat conductivity in the soil and hence water vapor exchange and heat flux between the land surface and the at-

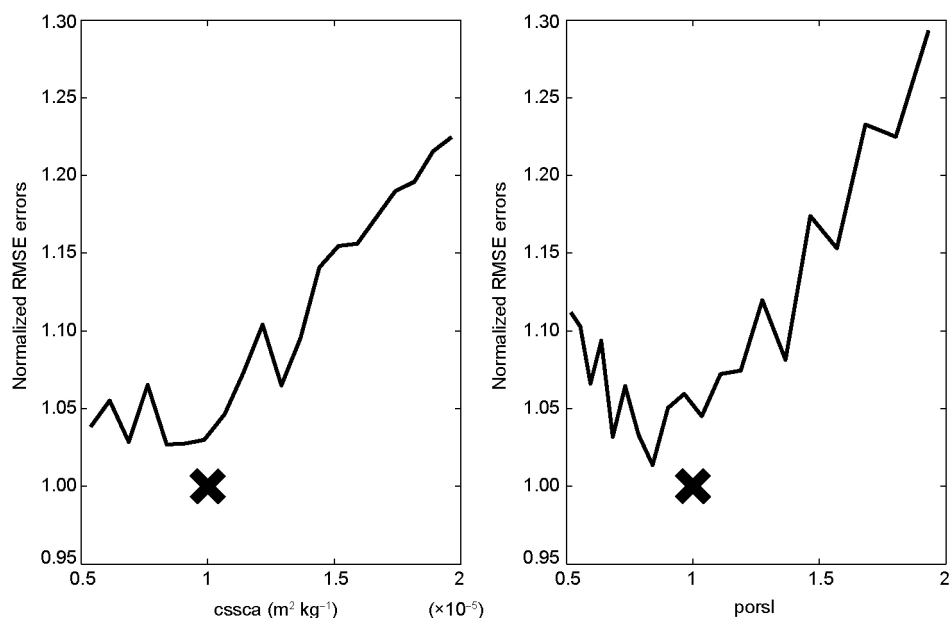


Figure 13 Response of 3-hourly average temperature to the two sensitive parameters in 180 simulations compared with observed data.

mosphere, which are important factors in the formation of convection precipitation. P16 (profile shape exponent used to calculate the momentum diffusivity coefficient) from the planetary boundary-layer scheme is a sensitive parameter for precipitation. Because it controls the mixing intensity of turbulent eddies in the planetary boundary layer, the upward transfer energy of water vapor and heat will change as P16 varies, affecting the development of convection.

4. Discussion and conclusions

This study has systematically examined the sensitivity of eighteen parameters from six parameterization schemes corresponding to six physical processes to high-resolution precipitation and temperature simulation results obtained by the Weather Research and Forecasting model, version 3.6.1. The parameter sampling approach used was QMC. Two types of SA experiments were performed. The first was qualitative SA using three methods (DT, MARS, and SOT), and the second was quantitative SA using the MARS response surface model-based Sobol' method. Qualitative SA obtained sensitivity rankings for parameters with fewer samples, whereas quantitative SA obtained accurate contribution percentages of parameters to the total variance of the WRF model response. For this reason, SA results from quantitative methods are generally used to validate SA results from qualitative methods.

It is well known that quantitative methods require simulation of tens of thousands of samples. Therefore, very few quantitative SA experiments have been performed for the complex NWP model because of its huge computational cost, resulting in a lack of validation for SA results. In this study,

one quantitative SA method, the MARS response surface model-based Sobol' method, was used to conduct a parametric SA of the WRF model. The results of the parametric SA obtained by the MARS response surface model-based Sobol' method were then used to validate the reasonableness of the qualitative SA. In addition, rather than using a single qualitative SA method, three qualitative SA methods were used to obtain more robust results for the sensitive parameters. In summary, qualitative and quantitative methods were used to perform a systematic evaluation of parametric SA of the WRF model for precipitation and temperature simulations, making the results for the sensitive parameters more accurate and reliable.

The first step was to use a QMC sampling approach to produce 180 relatively uniform samples from the high-dimensional parameter space. Then the simulated precipitation and temperature results from the WRF model with 180 perturbed parameter values were evaluated using the respective WRF simulations with default parameters as reference data. Finally, three qualitative methods and one quantitative method were applied to 180 combinations of perturbed parameters and their corresponding simulation errors. In the case of precipitation, the three qualitative SA methods identified four common sensitive parameters (P5, P7, P10, and P16), and the quantitative method added P3 to this list. Therefore, the five sensitive parameters were identified by both qualitative and quantitative methods. A two-way interactive effect between P7 and P10 was also evaluated as important to the output variance according to the relative contribution ratio of parametric main effects and interactive effects. The accumulated contribution ratios of the sensitive parameters for precipitation ranged from 76% for light rain to 90% for moderate rain for

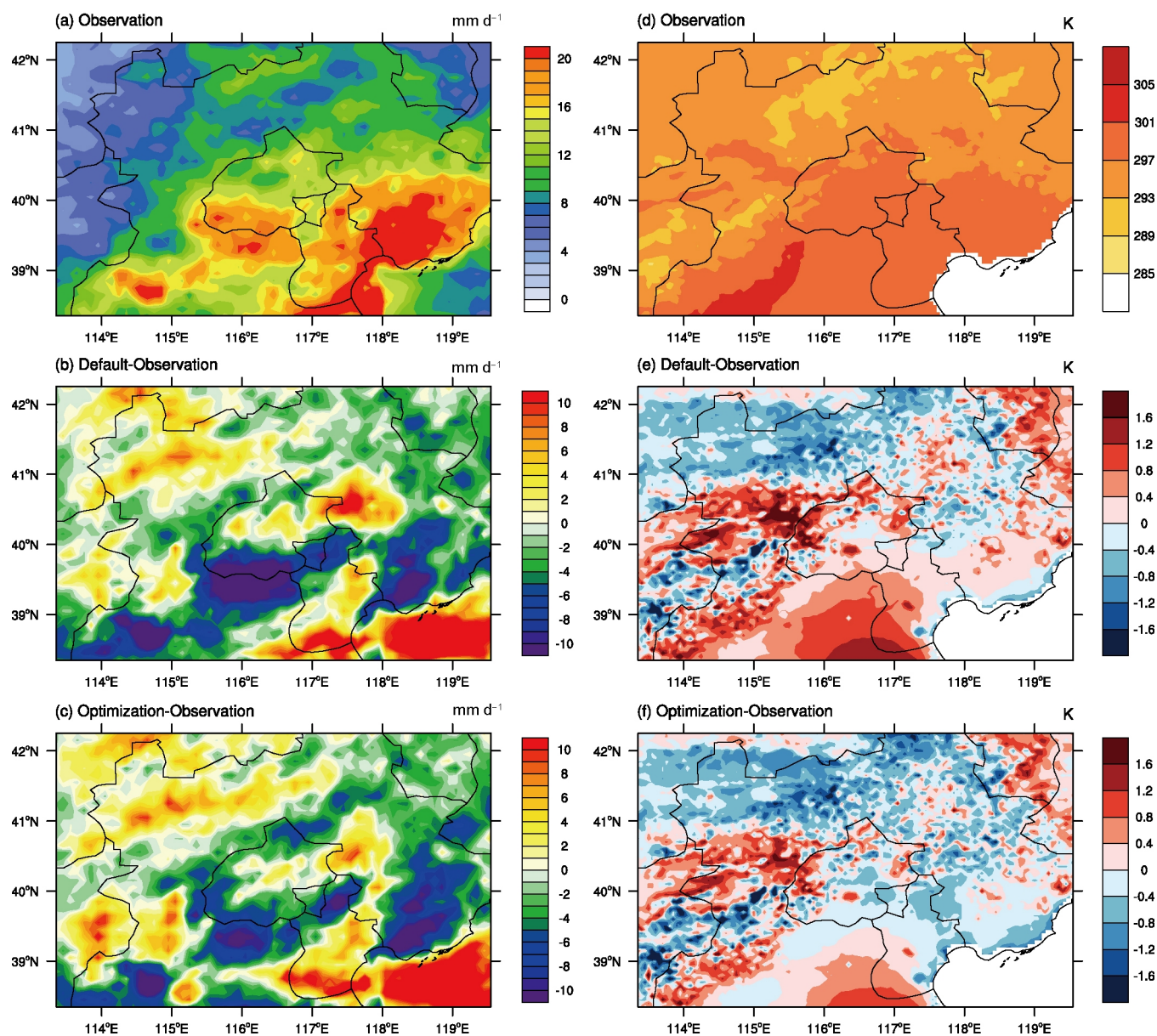


Figure 14 Comparison of simulated daily average precipitation (temperature) using default versus optimal parameter values for the nine two-day rainy (sunny) events during the summer season from 2008 to 2010.

6-hourly accumulated precipitation and from 84% for RMSE to 95.2% for heavy rain for 24-hourly accumulated precipitation, except for a 54% value for storm. For temperature, the same SA methods were used to conduct a parametric SA. The results showed that the common sensitive parameters were P7 and P10. There was less interactive effect (less than 5.3%) between P7 and P10, except for 24-hourly maximum temperature (approximately 29%). Overall, the accumulated contribution ratios of P7 and P10 for 3-hourly average, 24-hourly average, 24-hourly maximum, and 24-hourly minimum temperature were 95%, 79%, 84%, and 91%, respectively. In the last phase of this research, a preliminary exploration of precipitation and temperature optimization was performed by searching the sensitive parameter values, further proving that

the identification of the screened sensitive parameters was reasonable and reliable.

An integrated SA analysis strategy for WRF parameters, including qualitative parametric screening and quantitative parametric sensitivity evaluation, has been presented in this study, providing an effective solution for evaluating the parameter sensitivity of other models, especially for large, complex system models. However, the method proposed in this study has some limitations. For example, uncertainties in the initial and boundary conditions were not considered. The preliminary parametric optimization validated the robustness of the identification of the screened sensitive parameters by both qualitative and quantitative methods, but real parameter optimization was not conducted. Future studies will focus on

optimizing the sensitive parameters of the WRF precipitation model to explore parametric optimization strategies for large, complex dynamic models.

Acknowledgements We acknowledge the CFSR forcing dataset obtained from (<http://nomads.nccp.noaa.gov/modeldata/>), the validation data from the China Hourly Merged Precipitation Analysis precipitation products (CHMPA-Hourly, version 1.0, <http://cdc.nmic.cn/dataSetDetailed.do>), and the temperature data (<http://globalchange.bnu.edu.cn/research/forcing>). This research was supported by the Special Fund for Meteorological Scientific Research in the Public Interest (Grant No. GYHY201506002, CRA-40: 40-year CMA global atmospheric reanalysis), the National Basic Research Program of China (Grant No. 2015CB953703), the Intergovernmental Key International S & T Innovation Cooperation Program (Grant No. 2016YFE0102400), and the National Natural Science Foundation of China (Grant Nos. 41305052 & 41375139).

References

- Allen M. 1999. Do-it-yourself climate prediction. *Nature*, 401: 642–642
- Allen M R, Stott P A, Mitchell J F B, Schnur R, Delworth T L. 2000. Quantifying the uncertainty in forecasts of anthropogenic climate change. *Nature*, 407: 617–620
- Annan J D, Lunt D J, Hargreaves J C, Valdes P J. 2005. Parameter estimation in an atmospheric GCM using the Ensemble Kalman filter. *Nonlin Processes Geophys*, 12: 363–371
- Barker D M, Huang W, Guo Y R, Bourgeois A J, Xiao Q N. 2004. A three-dimensional variational data assimilation system for MM5: Implementation and initial results. *Mon Weather Rev*, 132: 897–914
- Bellprat O, Kotlarski S, Lüthi D, Schär C. 2012. Objective calibration of regional climate models. *J Geophys Res*, 117: D23115
- Bontoux P, Gilly B, Roux B. 1980. Analysis of the effect of boundary conditions on numerical stability of solutions of Navier-Stokes equations. *J Comp Phys*, 36: 417–427
- Box G E P, Behnken D W. 1960. Some new three level designs for the study of quantitative variables. *Technometrics*, 2: 455–475
- Box G E, Wilson W B. 1951. On the experimental attainment of optimum conditions. *J Roy Stat Soc B*, 13: 1–45
- Box G E, Hunter J S, Hunter W G. 2005. *Statistics for Experimenters: Design, Innovation, and Discovery*. New York: Wiley-Interscience
- Breiman L, Friedman J, Stone C J, Olshen R A. 1984. *Classification and Regression Trees*. Boca Raton (FL): CRC Press
- Caffisch R E. 1998. Monte Carlo and Quasi-Monte Carlo methods. *Acta Numer*, 7: 1–49
- Carter G M, Dallavalle J P, Glahn H R. 1989. Statistical forecasts based on the national meteorological center's numerical weather prediction system. *Weather Forecast*, 4: 401–412
- Charney J G. 1951. *Dynamic Forecasting by Numerical Process in Compendium of Meteorology*. Boston: American Meteorological Society
- Charlton A J, Oneill A, Lahoz W A, Massacand A C. 2004. Sensitivity of tropospheric forecasts to stratospheric initial conditions. *Q J R Meteorol Soc*, 130: 1771–1792
- Chen F, Dudhia J. 2001. Coupling an advanced land surface-hydrology model with the Penn State-NCAR MM5 modeling system. Part I: Model implementation and sensitivity. *Mon Weather Rev*, 129: 569–585
- Chen F, Kusaka H, Bornstein R, Ching J, Grimmond C S B, Grossman-Clarke S, Loridan T, Manning K W, Martilli A, Miao S, Sailor D, Salamanca F P, Taha H, Tewari M, Wang X, Wysogrodzki A A, Zhang C. 2011. The integrated WRF/urban modelling system: Development, evaluation, and applications to urban environmental problems. *Int J Climatol*, 31: 273–288
- Chen F, Liu C, Dudhia J, Chen M. 2014. A sensitivity study of high-resolution regional climate simulations to three land surface models over the western United States. *J Geophys Res-Atmos*, 119: 7271–7291
- Chou M D, Suarez M J. 1994. An efficient thermal infrared radiation parameterization for use in general circulation models. NASA Tech Memo, 104606: 1–85
- Collins M, Allen M R. 2002. Assessing the relative roles of initial and boundary conditions in interannual to decadal climate predictability. *J Clim*, 15: 3104–3109
- Danforth C M, Kalnay E, Miyoshi T. 2007. Estimating and correcting global weather model error. *Mon Weather Rev*, 135: 281–299
- Di Z, Duan Q, Gong W, Wang C, Gan Y, Quan J, Li J, Miao C, Ye A, Tong C. 2015. Assessing WRF model parameter sensitivity: A case study with 5 day summer precipitation forecasting in the Greater Beijing Area. *Geophys Res Lett*, 42: 579–587
- Dudhia J. 1989. Numerical study of convection observed during the winter monsoon experiment using a mesoscale two-dimensional model. *J Atmos Sci*, 46: 3077–3107
- Dudhia J, Gill D, Guo Y R, Manning K, Wang W, Chriszar J. 2001. PSU/NCAR Mesoscale Modeling System Tutorial Class Notes and User Guide: MM5 Modeling System Version 3
- Eiroa E, Liitiäinen E, Lendasse A, Corona F, Verleysen M. 2008. Using the delta test for variable selection. In: *European Symposium on Artificial Neural Networks*. Bruges. 25–30
- Friedman J H. 1991. Multivariate adaptive regression splines. *Ann Statist*, 19: 1–67
- Gilliam R C, Pleim J E. 2010. Performance assessment of new land surface and planetary boundary layer physics in the WRF-ARW. *J Appl Meteorol Climatol*, 49: 760–774
- Gilmore M S, Straka J M, Rasmussen E N. 2004. Precipitation uncertainty due to variations in precipitation particle parameters within a simple microphysics scheme. *Mon Weather Rev*, 132: 2610–2627
- Glahn H R, Lowry D A. 1972. The use of model output statistics (MOS) in objective weather forecasting. *J Appl Meteorol*, 11: 1203–1211
- Gong W, Duan Q, Li J, Wang C, Di Z, Dai Y, Ye A, Miao C. 2015. Multi-objective parameter optimization of common land model using adaptive surrogate modeling. *Hydrol Earth Syst Sci*, 19: 2409–2425
- Grell G A, Dévényi D. 2002. A generalized approach to parameterizing convection combining ensemble and data assimilation techniques. *Geophys Res Lett*, 29: 38-1–38-4
- Halton J H, Smith G B. 1964. Algorithm 247: Radical-inverse quasi-random point sequence. *Commun ACM*, 7: 701–702
- Hong S Y, Dudhia J, Chen S H. 2004. A revised approach to ice microphysical processes for the bulk parameterization of clouds and precipitation. *Mon Weather Rev*, 132: 103–120
- Hong S Y, Lim J O J. 2006. The WRF single-moment 6-class microphysics scheme (WSM6). *J Korean Meteorol Soc*, 42: 129–151
- Hong S Y, Noh Y, Dudhia J. 2006. A new vertical diffusion package with an explicit treatment of entrainment processes. *Mon Weather Rev*, 134: 2318–2341
- Hong S Y, Pan H L. 1996. Nonlocal boundary layer vertical diffusion in a medium-range forecast model. *Mon Weather Rev*, 124: 2322–2339
- Hou Z, Huang M, Leung L R, Lin G, Ricciuto D M. 2012. Sensitivity of surface flux simulations to hydrologic parameters based on an uncertainty quantification framework applied to the Community Land Model. *J Geophys Res*, 117: D15108
- Hou Z, Rubin Y. 2005. On minimum relative entropy concepts and prior compatibility issues in vadose zone inverse and forward modeling. *Water Resour Res*, 41: W12425
- Huang C, Zheng X, Tait A, Dai Y, Yang C, Chen Z, Li T, Wang Z. 2014. On using smoothing spline and residual correction to fuse rain gauge observations and remote sensing data. *J Hydrol*, 508: 410–417
- Huang X Y, Xiao Q, Barker D M, Zhang X, Michalakes J, Huang W, Henderson T, Bray J, Chen Y, Ma Z, Dudhia J, Guo Y, Zhang X, Won D J, Lin H C, Kuo Y H. 2009. Four-dimensional variational data assimilation for wrf: Formulation and preliminary results. *Mon Weather*

- Rev, 137: 299–314
- Jackson C, Sen M K, Stoffa P L. 2004. An efficient stochastic bayesian approach to optimal parameter and uncertainty estimation for climate model predictions. *J Clim*, 17: 2828–2841
- Jia B, Tian X, Xie Z, Liu J, Shi C. 2013. Assimilation of microwave brightness temperature in a land data assimilation system with multi-observation operators. *J Geophys Res Atmos*, 118: 3972–3985
- Johannesson G, Lucas D, Qian Y, Swiler L P, Wildey T M. 2014. Sensitivity of precipitation to parameter values in the Community Atmosphere Model Version 5, SAND2014-0829. Albuquerque, NM: Sandia National Laboratories
- Kain J S. 2004. The Kain-Fritsch convective parameterization: An update. *J Appl Meteorol*, 43: 170–181
- Kenny Q Y, Li W, Sudjianto A. 2000. Algorithmic construction of optimal symmetric Latin hypercube designs. *J Stat Plann Infer*, 90: 145–159
- Kim J C, Lee C B, Belorid M, Zhao P. 2011. A study of sensitivity of WRF simulation to microphysics parameterizations, slope option and analysis nudging in Haean Basin, South Korea. In: TERRECO Science Conference. Germany: Karlsruhe Inst of Tech
- Kondrashov D, Sun C, Ghil M. 2008. Data assimilation for a coupled ocean-atmosphere model. Part II: Parameter estimation. *Mon Weather Rev*, 136: 5062–5076
- Knutti R, Stocker T F, Joos F, Plattner G K. 2002. Constraints on radiative forcing and future climate change from observations and climate model ensembles. *Nature*, 416: 719–723
- Kusaka H, Kimura F. 2004. Coupling a single-layer urban canopy model with a simple atmospheric model: Impact on urban heat island simulation for an idealized case. *J Meteorol Soc Jpn*, 82: 67–80
- Liu J, Bray M, Han D. 2013. Exploring the effect of data assimilation by WRF-3DVar for numerical rainfall prediction with different types of storm events. *Hydrol Process*, 27: 3627–3640
- Liu Y, Gupta H V, Sorooshian S, Bastidas L A, Shuttleworth W J. 2004. Exploring parameter sensitivities of the land surface using a locally coupled land-atmosphere model. *J Geophys Res*, 109: D21101
- Lorenz E N. 1963. Deterministic nonperiodic flow. *J Atmos Sci*, 20: 130–141
- Mckay M D, Beckman R J, Conover W J. 2000. A comparison of three methods for selecting values of input variables in the analysis of output from a computer code. *Technometrics*, 42: 55–61
- Medvigy D, Walko R L, Otte M J, Avissar R. 2010. The ocean-land-atmosphere model: Optimization and evaluation of simulated radiative fluxes and precipitation. *Mon Weather Rev*, 138: 1923–1939
- Mlawer E J, Taubman S J, Brown P D, Iacono M J, Clough S A. 1997. Radiative transfer for inhomogeneous atmospheres: RRTM, a validated correlated-k model for the longwave. *J Geophys Res*, 102: 16663–16682
- Nasrollahi N, AghaKouchak A, Li J, Gao X, Hsu K, Sorooshian S. 2012. Assessing the impacts of different WRF precipitation physics in hurricane simulations. *Wea Forecasting*, 27: 1003–1016
- Niska H, Rantamäki M, Hiltunen T, Karppinen A, Kukkonen J, Ruuskanen J, Kolehmainen M. 2005. Evaluation of an integrated modelling system containing a multi-layer perceptron model and the numerical weather prediction model HIRLAM for the forecasting of urban airborne pollutant concentrations. *Atmos Environ*, 39: 6524–6536
- Nitta T, Ogura Y. 1972. Numerical simulation of the development of the intermediate-scale cyclone in a moist model atmosphere. *J Atmos Sci*, 29: 1011–1025
- Orrell D, Smith L, Barkmeijer J, Palmer T N. 2001. Model error in weather forecasting. *Nonlin Processes Geophys*, 8: 357–371
- Pleim J E. 2006. A simple, efficient solution of flux-profile relationships in the atmospheric surface layer. *J Appl Meteorol Climatol*, 45: 341–347
- Qian Y, Yan H, Hou Z, Johannesson G, Klein S, Lucas D, Neale R, Rasch P, Swiler L, Tannahill J, Wang H, Wang M, Zhao C. 2015. Parametric sensitivity analysis of precipitation at global and local scales in the Community Atmosphere Model CAM5. *J Adv Model Earth Syst*, 7: 382–411
- Qiu C, Chou J. 1988. A new approach to improve the numerical weather prediction. *Sci China Ser B*, 31: 1132–1142
- Ruiz J, Ferreira L, Saulo C. 2007. WRF-ARW sensitivity to different planetary boundary layer parameterization over South America. 4-11, 4-12 Research activities in atmospheric and oceanic modelling. In: WGNE Blue Book, WMO
- Saltelli A, Chan K, Scott E M. 2000. Sensitivity Analysis. New York: John Wiley & Sons
- Saltelli A, Tarantola S, Campolongo F, Ratto M. 2004. Sensitivity Analysis in Practice: A guide to Assessing Scientific Models. New York: John Wiley & Sons
- Schirber S, Klocke D, Pincus R, Quaas J, Anderson J L. 2013. Parameter estimation using data assimilation in an atmospheric general circulation model: From a perfect toward the real world. *J Adv Model Earth Syst*, 5: 58–70
- Shahsavani D, Tarantola S, Ratto M. 2010. Evaluation of MARS modeling technique for sensitivity analysis of model output. *Proc Soc Behavior Sci*, 2: 7737–7738
- Shen Y, Zhao P, Pan Y, Yu J. 2014. A high spatiotemporal gauge-satellite merged precipitation analysis over China. *J Geophys Res-Atmos*, 119: 3063–3075
- Skamarock W, Klemp J, Dudhia J, Gill D, Barker D, Duda M, Huang X, Wang W, Powers J. 2008. A description of the Advanced Research WRF Version 3, NCAR technical note. Boulder: Mesoscale and Microscale Meteorology Division, National Center for Atmospheric Research
- Sobol' I M. 1967. On the distribution of points in a cube and the approximate evaluation of integrals. *USSR Comp Math Math Phys*, 7: 86–112
- Sobol' I M. 1993. Sensitivity analysis for nonlinear mathematical models. *Math Mod Comput Exp*, 1: 407–414
- Sobol' I M. 2001. Global sensitivity indices for nonlinear mathematical models and their Monte Carlo estimates. *Math Comp Simulation*, 55: 271–280
- Solonen A, Ollinaho P, Laine M, Haario H, Tamminen J, Järvinen H. 2012. Efficient MCMC for climate model parameter estimation: Parallel adaptive chains and early rejection. *Bayesian Anal*, 7: 715–736
- Steinberg D, Colla P, Martin K. 1999. MARS User Guide. San Diego: Salford Systems
- Stephens G L, Ackerman S, Smith E A. 1984. A shortwave parameterization revised to improve cloud absorption. *J Atmos Sci*, 41: 687–690
- Sun Q, Xie Z H, Tian X J. 2015. GRACE terrestrial water storage data assimilation based on the ensemble four-dimensional variational method PO-DEn4DVar: Method and validation. *Sci China Earth Sci*, 58: 371–384
- Tang Y, Reed P, Wagener T, van Werkhoven K. 2007. Comparing sensitivity analysis methods to advance lumped watershed model identification and evaluation. *Hydrol Earth Syst Sci*, 11: 793–817
- Thompson G, Field P R, Rasmussen R M, Hall W D. 2008. Explicit forecasts of winter precipitation using an improved bulk microphysics scheme. Part II: Implementation of a new snow parameterization. *Mon Weather Rev*, 136: 5095–5115
- van Werkhoven K, Wagener T, Reed P, Tang Y. 2009. Sensitivity-guided reduction of parametric dimensionality for multi-objective calibration of watershed models. *Adv Water Resources*, 32: 1154–1169
- Villagran A, Huerta G, Jackson C S, Sen M K. 2008. Computational methods for parameter estimation in climate models. *Bayesian Anal*, 3: 823–850
- Walko R L, Cotton W R, Meyers M P, Harrington J Y. 1995. New RAMS cloud microphysics parameterization part I: The single-moment scheme. *Atmos Res*, 38: 29–62
- Wang C, Duan Q, Gong W, Ye A, Di Z, Miao C. 2014. An evaluation of adaptive surrogate modeling based optimization with two benchmark problems. *Environ Model Softw*, 60: 167–179
- Wang C, Duan Q, Tong C H, Di Z, Gong W. 2016. A GUI platform for uncertainty quantification of complex dynamical models. *Environ Model Softw*, 76: 1–12
- Wang X, Barker D M, Snyder C, Hamill T M. 2008. A Hybrid ETKF-3DVAR

- data assimilation scheme for the WRF Model. Part I: Observing system simulation experiment. *Mon Weather Rev*, 136: 5116–5131
- Woodbury A D, Ulrych T J. 1993. Minimum relative entropy: Forward probabilistic modeling. *Water Resour Res*, 29: 2847–2860
- Yang B, Qian Y, Lin G, Leung R, Zhang Y. 2012. Some issues in uncertainty quantification and parameter tuning: A case study of convective parameterization scheme in the WRF regional climate model. *Atmos Chem Phys*, 12: 2409–2427
- Yang B, Zhang Y, Qian Y, Wu T, Huang A, Fang Y. 2015. Parametric sensitivity analysis for the asian summer monsoon precipitation simulation in the Beijing climate center AGCM, version 2.1. *J Clim*, 28: 5622–5644
- Zhang D L, Fritsch J M. 1986. A case study of the sensitivity of numerical simulation of mesoscale convective systems to varying initial conditions. *Mon Weather Rev*, 114: 2418–2431
- Ziehn T, Tomlin A S. 2009. GUI-HDMR—A software tool for global sensitivity analysis of complex models. *Environ Model Softw*, 24: 775–785
- Zou L, Qian Y, Zhou T, Yang B. 2014. Parameter tuning and calibration of RegCM3 with MIT-Emanuel cumulus parameterization scheme over CORDEX East Asia domain. *J Clim*, 27: 7687–7701
- Zou X, Kuo Y H. 1996. Rainfall assimilation through an optimal control of initial and boundary conditions in a limited-area mesoscale model. *Mon Weather Rev*, 124: 2859–2882